Science Advances
AAAS

advances.sciencemag.org/cgi/content/full/7/20/eabf3985/DC1

Supplementary Materials for

Changes in plant-herbivore network structure and robustness along land-use intensity gradients in grasslands and forests

Felix Neff*, Martin Brändle, Didem Ambarlı, Christian Ammer, Jürgen Bauhus, Steffen Boch, Norbert Hölzel, Valentin H. Klaus, Till Kleinebecker, Daniel Prati, Peter Schall, Deborah Schäfer, Ernst-Detlef Schulze, Sebastian Seibold, Nadja K. Simons, Wolfgang W. Weisser, Loïc Pellissier, Martin M. Gossner

*Corresponding author. Email: felix.neff@wsl.ch

Published 14 May 2021, *Sci. Adv.* **7**, eabf3985 (2021)
DOI: 10.1126/sciadv.abf3985

This PDF file includes:

Supplementary Text

Additional sensitivity analyses

Based on the basic equation 1 in the main manuscript, different inputs were used to correct for four potential biases in our models:

(i) *Feeding type*. Some species recorded are only facultative herbivores and might also feed on other food sources such as other insects. Based on literature data on feeding habits (*68*), insect abundance N_{ip} was reduced by a factor of 0.5 for omnivorous species and 0.25 for all other species mainly feeding as e.g., carnivores.

(ii) *Information accuracy*. Information in the interaction database is at different taxonomic levels for the plants. To weight taxonomically more precise information stronger, the interaction dummy parameter *a* was reduced to 0.5 for information higher than the genus level and to 0.25 for information higher than the family level, including rough information on plant groups (e.g., "forbs") only.

(iii) *Metabolic rate*. To account for differences in body size, which might affect interaction strength through changes in metabolic rates (*69*), the body mass of all insect species was calculated based on their body length, which was estimated from the literature (*68*). To determine body mass w_i of insect species *I*, allometric relationships of the form

$$w_i = \alpha_{0i} \cdot l_i^{\alpha_{1i}} \quad (6)$$

were used, where l_i is the mean body length of insect species *i* and α_{0i}, α_{1i} are empirical parameters, which were estimated from data that were recently published for a variety of temperate insect species (*70*, *71*). To minimize errors originating from differences in body form, the lowest taxonomic level covered in ref. (*71*) was used for all study species for parameter estimation. Finally, following ref. (*72*), the relative population metabolic rate R_{ip} of insect species *i* in a plot *p* was determined as

$$R_{ip} = N_{ip} \cdot w_i^{3/4} \quad (7)$$

where N_{ip} is the total abundance of insect species *i* in plot *p* and w_i is the estimated biomass of an individual of insect species *i*. *N* in equation 1 was then substituted with *R*.

(iv) *Plant biomass*. Using plant cover for network construction might also lead to biased results because plants differ in their biomass per area and thus provide different amounts of food for insect herbivores per unit area. Thus, plant biomass was estimated using two different approaches in forests and grasslands. In forests, biomass was separately estimated for non-tree species, trees shorter than 1.3 m and trees larger than 1.3 m. For non-tree species, total aboveground biomass was estimated based on plant cover, which was recorded in the vegetation surveys, and literature-based mean height (*73*) with a set of allometric equations developed for understory plants in temperate forests (*74*). For trees shorter than 1.3 m, data was taken from an inventory of short tree regeneration, which was carried out in 25 circles of 1 m radius on all plots (2014–2016). In the inventory trees were recorded for different height classes, and this data was used to estimate approximate cover values per tree species. From reported height and cover, total aboveground biomass was then estimated using the same kind of allometric equations as used for non-tree species (*75*). For trees higher than 1.3 m, tree-specific data from the forest and regeneration inventories mentioned above was used to estimate total mass of foliage, which is the main food source for most of the herbivores encountered in this study. Foliage mass was estimated from diameter at breast height using a set of allometric equations (*76*). Finally, all three biomass components were standardized per area and summed, yielding total biomass M for each plant species and plot. For grasslands, a simpler approach was used and biomass M of each plant species was estimated by multiplying the recorded cover in each plot with literature-based mean plant height (*73*). For both ecosystems, the estimated biomass M was then included in equation 1 in place of plant cover C.

Networks were constructed for all corrections, as well as all possible combinations of the corrections, and the analyses along land-use intensity gradients were performed for every case. Results are given in figs S8–S10 and S15–S17.

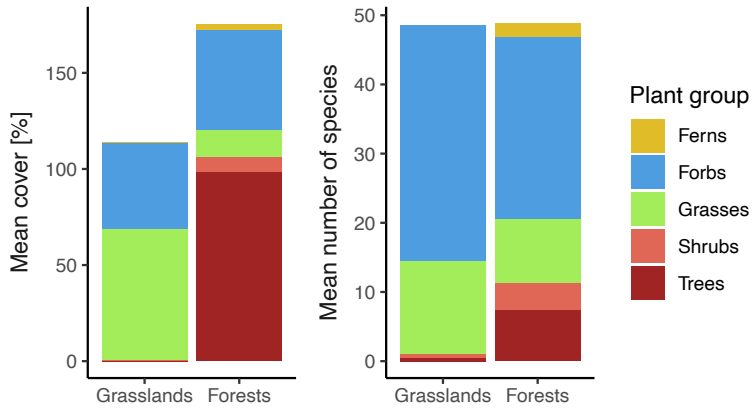

Fig. S1.

Mean plant community composition of study plots, separated by ecosystem (grasslands, forests) and by plant functional group. The left graph shows mean area cover values. Values can exceed 100% because cover was not standardized to sum 100% and different cover layer overlap. The right graph shows the mean number of plant species recorded in 4 × 4 m^2 subplots in grasslands and in 20 × 20 m^2 subplots (plants up to 5 m high) or the whole 100 × 100 m^2 plots (plants higher than 5 m) in forests.

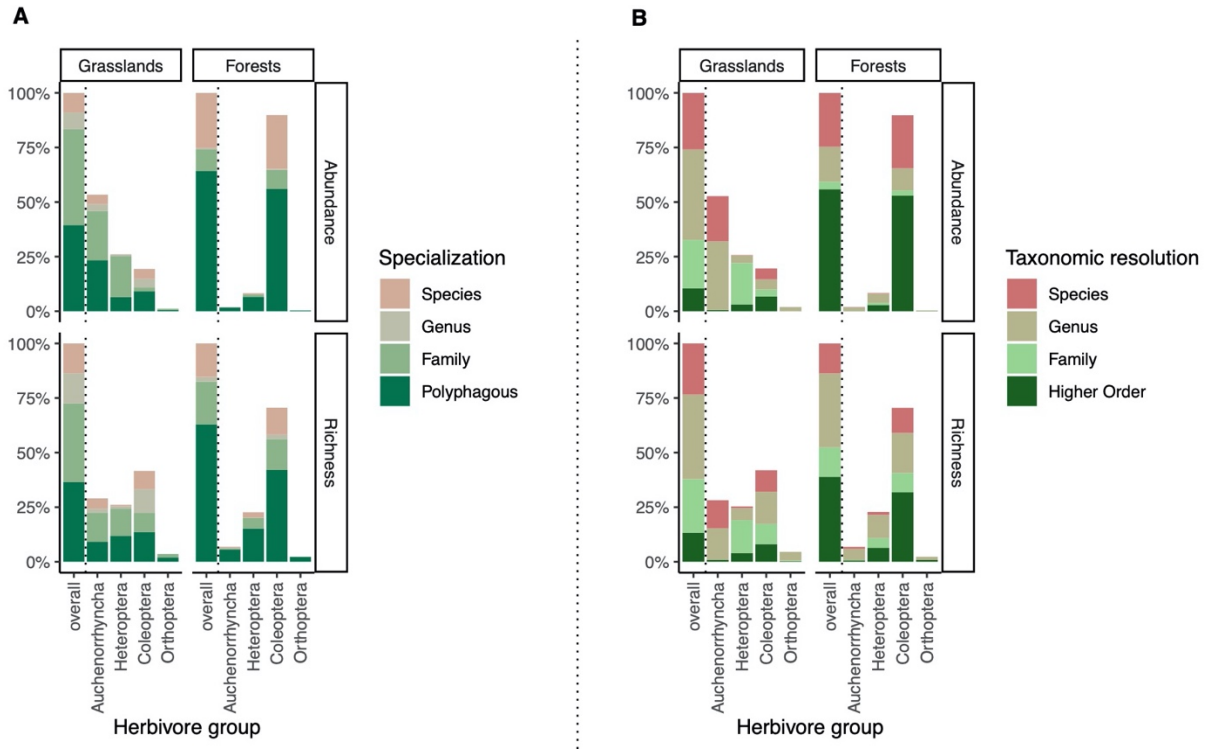

Fig. S2.

Mean herbivore community composition in grasslands and forests for the overall community and for the different herbivore groups. Community composition is shown based on total abundances and on species richness. (**A**) Species grouped by specialization, which was categorized according to the taxonomic range of food plants recorded for a herbivore species within each ecosystem. Species feeding on several plant families were categorized as polyphagous. (**B**) Species grouped by the taxonomic resolution of the food plants in the interaction database, i.e., the highest taxonomic rank reported for a herbivore species. The category *Higher Order* includes any information at taxonomic levels higher than family, as well as information for plant groups only (e.g., 'trees'). The herbivore community in forests mainly consisted of Coleoptera (89.8 ± 5.5% of individuals), whereas in grasslands Auchenorrhyncha (52.7 ± 18.6%), Heteroptera (25.8 ± 12.3%) and Coleoptera (19.6 ± 13.2%) made up major shares of the community. This is probably due to more species being bound to herbaceous plants in the investigated hemipteran groups (Auchenorrhyncha, Heteroptera), which might have evolutionary reasons (*77*). These compositional differences, as well as differences in specialization between the two ecosystems within insect orders, resulted in a higher proportion of polyphagous species in forests compared with grasslands. Various mechanisms related to evolutionary or ecological factors could explain this difference in herbivore feeding specialization. For example, more frequent disturbances in grasslands potentially increase the speed of eco-evolutionary dynamics (*78*), which could have resulted in a higher amount of specialized herbivores and thus higher modularity. At the same time, we observed higher evenness of plant abundance in grasslands, which could indicate that grasslands provide a more constant source of diverse food plants. This would allow more specialized herbivores to coexist, resulting in the observed differences between the studied ecosystems.

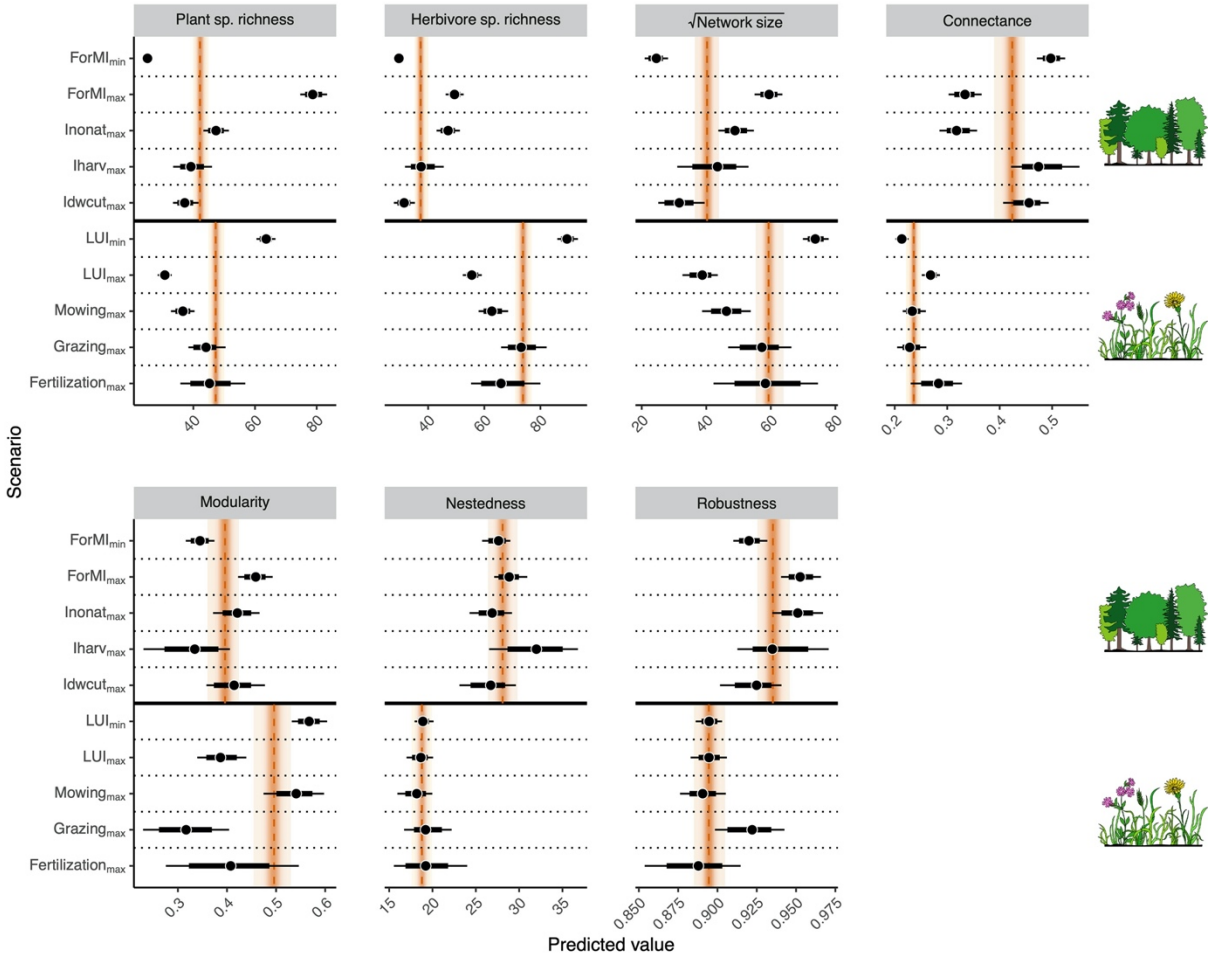

Fig. S3.

Based on hierarchical models on the relation of network metrics and land-use intensity, predictions for network metrics for a set of scenarios (black points and lines) are shown along with model intercepts corresponding to values at mean land-use intensity (orange lines and shaded areas). Results are shown for plant species richness, herbivore species richness, network size (i.e., plant species richness times herbivore species richness, square-root transformed), connectance, modularity, nestedness and robustness. For each ecosystem (grasslands, bottom; forests, top), one scenario was chosen at minimum and at maximum combined land-use intensity (LUI_{min}, LUI_{max} for grasslands and $ForMI_{min}$, $ForMI_{max}$ for forests). Additionally, there are scenarios for maximum observed values of each separate land-use component, while keeping the others minimal (*Inonat*: proportion of tree species that are not part of the natural community; *Iharv*: proportion of harvested wood volume; *Idwcut*: proportion of deadwood with saw cuts). Hierarchical models with Poisson-distributed response variables and a log-link function were used for analysis of species richness; hierarchical models with normally distributed response variables and an identity link function were used for analysis of all other metrics. Horizontal black thin lines show the 95% highest density interval (HDI), bold lines show the 77.6% HDI for all scenario predictions, and points show the highest maximum a posteriori estimates. No overlap of 77.6% HDIs between scenarios indicates a significant difference on the 5% level.

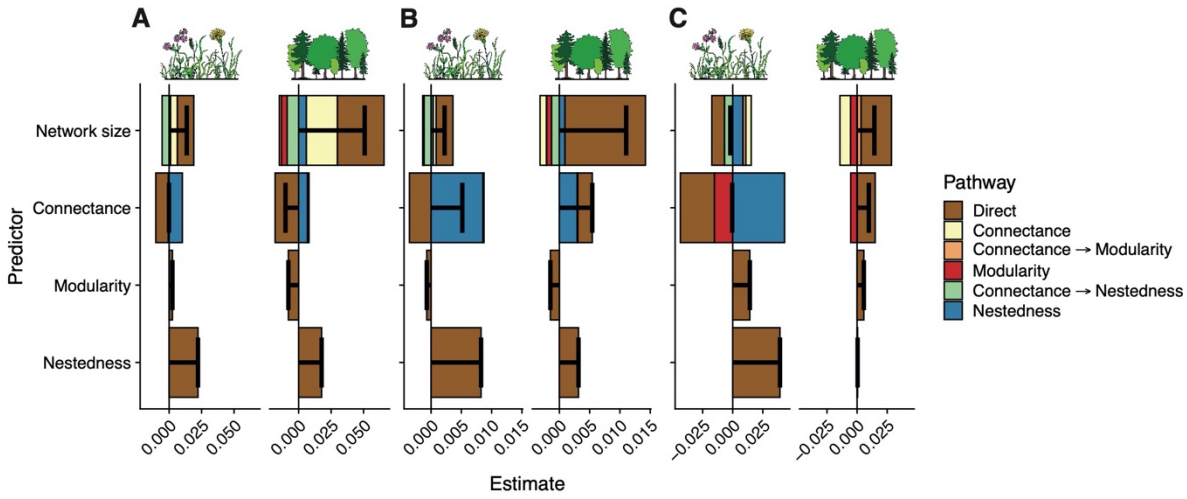

Fig. S4.

Summarized pathway estimates for all direct and indirect pathways linking network structure to network robustness, arranged by the different network structure metrics, analyzed with different sensitivity scenarios. (**A**) Imprecise interaction information was excluded from the interaction database (i.e., information higher than plant-family level); (**B**) all plant species were added in very small quantities to all plots (i.e., no herbivores excluded because of missing food sources); (**C**) interaction strength was not considered (i.e., presence–absence networks). Different structural equation models were used for grasslands (left) and forests (right). The intermediate variables linking predictors and robustness as well as direct pathways are indicated by the different colors. All potential pathways are shown in Fig. 3A. The overall effect of a predictor on robustness (i.e., sum of all direct and indirect pathways) is shown with the black bars. Note that all predictor variables were scaled to standard deviation 1 (across both ecosystems) prior to analyses to make pathway estimates comparable. Detailed results from structural equation modeling are given in table S2.

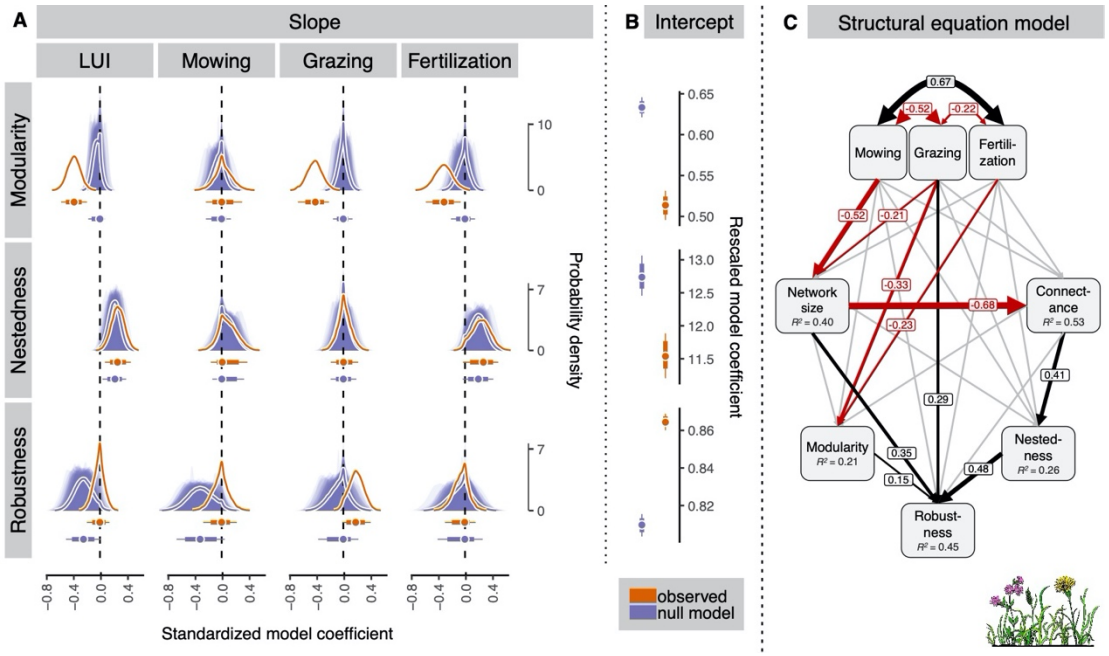

Fig. S5.

Grasslands: analyses for the case where imprecise interaction information was excluded from the interaction database (i.e., information higher than plant-family level). Posterior distributions of (**A**) slope estimates and (**B**) intercept estimates for the fixed effects from hierarchical models testing the effects of land-use intensity on network metrics in observed networks (orange) and null model networks (purple), in which network size and connectance were kept constant. Slope estimates are shown for models on combined land-use intensity (*LUI*) and for models on the single components of land-use intensity. Positive estimates indicate higher values at high land-use intensity. Intercept estimates correspond to overall means given that all variables were scaled. Intercepts were obtained from the model on the combined *LUI* index. Values were rescaled to the original metric scale. Curves show probability densities of the posterior distributions; thin lines show the 95% highest density interval (HDI), bold lines show the 77.6% HDI, and points show the highest maximum a posteriori estimates. No overlap of 77.6% HDIs between the observation and null model indicates a significant difference on the 5% level. Shaded purple areas show the posterior distributions for single null-model realizations (n = 100). (**C**) Results from piecewise structural equation models testing the effects of land-use intensity components on basic network metrics (network size, connectance), modularity and nestedness, and their relationship with robustness. Numbers show standardized path coefficients for significant pathways. Network size was square-root transformed prior to analyses. Positive paths are in black, negative in red, and non-significant in grey. R^2 values (conditional) for all variables are provided within the boxes. Fisher's $C = 5.77$, $P = 0.056$.

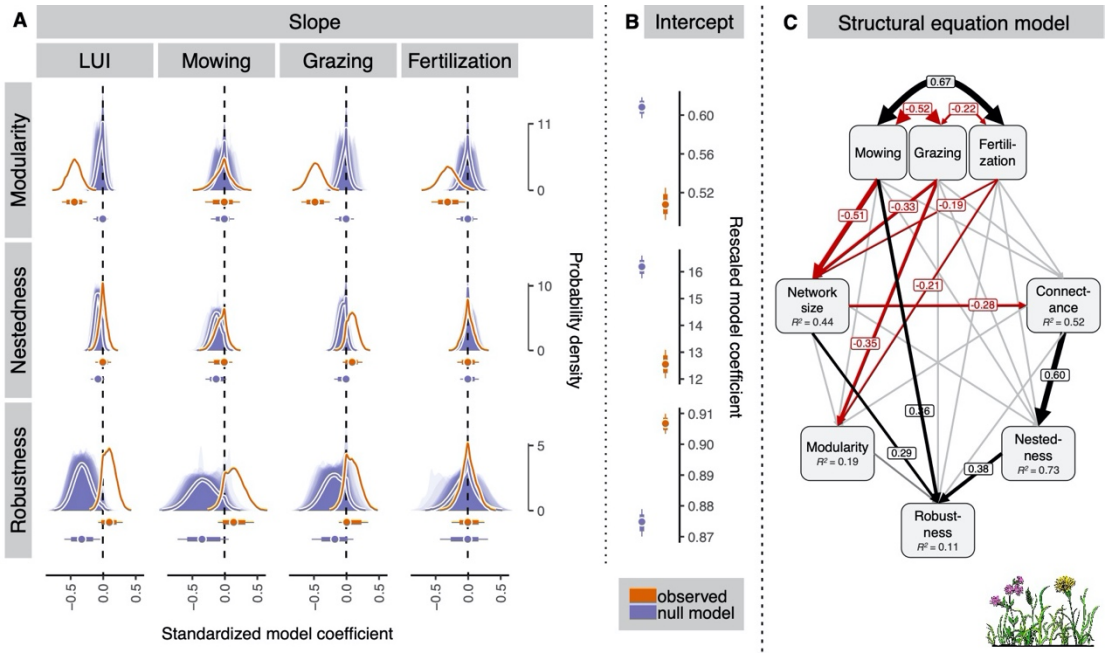

Fig. S6.

Grasslands: Analyses for the case where all plant species were added in very small quantities to all plots (i.e., no herbivores excluded because of missing food sources). Posterior distributions of (**A**) slope estimates and (**B**) intercept estimates for the fixed effects from hierarchical models testing the effects of land-use intensity on network metrics in observed networks (orange) and null model networks (purple), in which network size and connectance were kept constant. Slope estimates are shown for models on combined land-use intensity (*LUI*) and for models on the single components of land-use intensity. Positive estimates indicate higher values at high land-use intensity. Intercept estimates correspond to overall means given that all variables were scaled. Intercepts were obtained from the model on the combined *LUI* index. Values were rescaled to the original metric scale. Curves show probability densities of the posterior distributions; thin lines show the 95% highest density interval (HDI), bold lines show the 77.6% HDI, and points show the highest maximum a posteriori estimates. No overlap of 77.6% HDIs between the observation and null model indicates a significant difference on the 5% level. Shaded purple areas show the posterior distributions for single null-model realizations (n = 100). (**C**) Results from piecewise structural equation models testing the effects of land-use intensity components on basic network metrics (network size, connectance), modularity and nestedness, and their relationship with robustness. Numbers show standardized path coefficients for significant pathways. Network size was square-root transformed prior to analyses. Positive paths are in black, negative in red, and non-significant in grey. R^2 values (conditional) for all variables are provided within the boxes. Fisher's $C = 2.32$, $P = 0.314$.

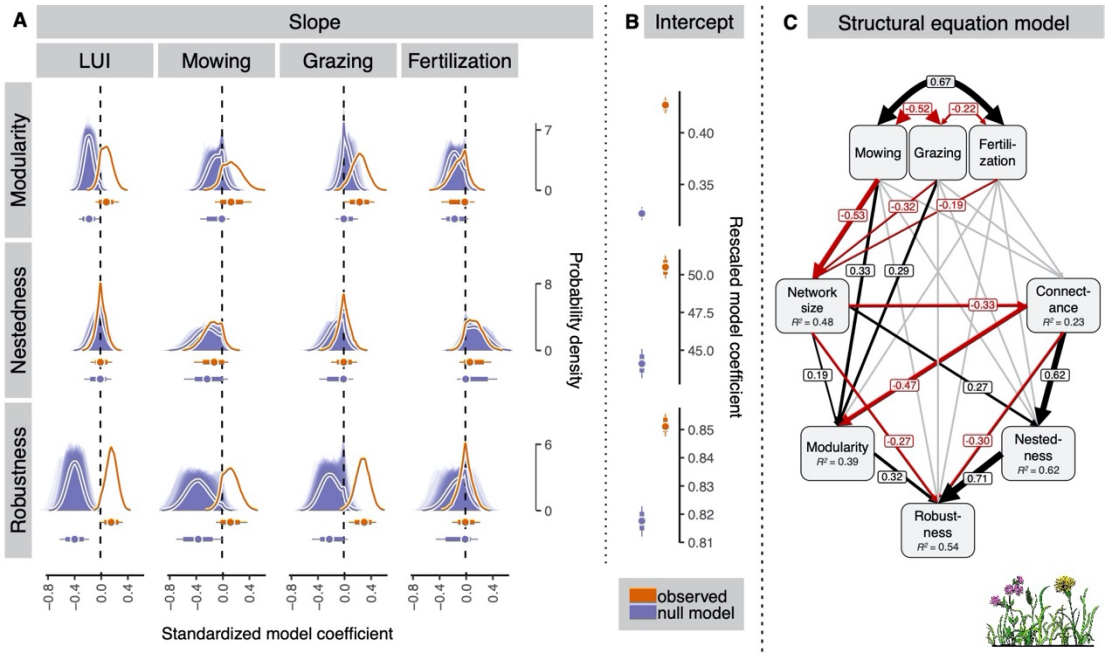

Fig. S7.

Grasslands: Analyses for the case where interaction strength was not considered (i.e., presence–absence networks). Posterior distributions of (**A**) slope estimates and (**B**) intercept estimates for the fixed effects from hierarchical models testing the effects of land-use intensity on network metrics in observed networks (orange) and null model networks (purple), in which network size and connectance were kept constant. Slope estimates are shown for models on combined land-use intensity (*LUI*) and for models on the single components of land-use intensity. Positive estimates indicate higher values at high land-use intensity. Intercept estimates correspond to overall means given that all variables were scaled. Intercepts were obtained from the model on the combined *LUI* index. Values were rescaled to the original metric scale. Curves show probability densities of the posterior distributions; thin lines show the 95% highest density interval (HDI), bold lines show the 77.6% HDI, and points show the highest maximum a posteriori estimates. No overlap of 77.6% HDIs between the observation and null model indicates a significant difference on the 5% level. Shaded purple areas show the posterior distributions for single null-model realizations (n = 100). (**C**) Results from piecewise structural equation models testing the effects of land-use intensity components on basic network metrics (network size, connectance), modularity and nestedness, and their relationship with robustness. Numbers show standardized path coefficients for significant pathways. Network size was square-root transformed prior to analyses. Positive paths are in black, negative in red, and non-significant in grey. R^2 values (conditional) for all variables are provided within the boxes. Fisher's $C = 2.8$, $P = 0.246$.

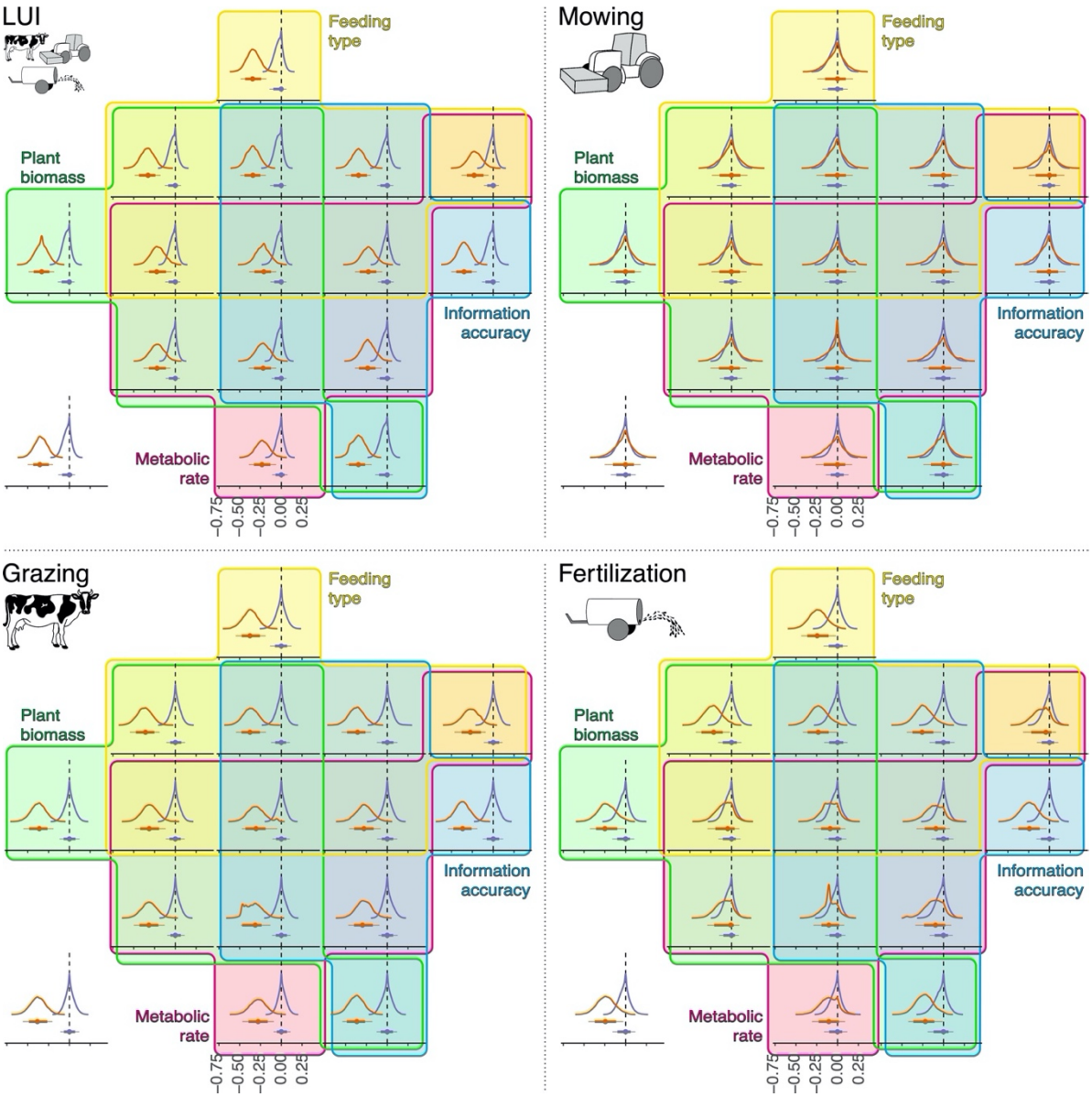

Fig. S8.

Grasslands: posterior distributions of slope estimates for models testing the effects of grassland land-use intensity on network modularity. Each panel relies on a different correction method or on a combination of several methods as indicated by the overlaid colored shapes, each of which is representing a correction method: feeding type – down-weighing of omnivorous insect species (yellow); information accuracy – downweighing of interactions with less precise information on food plants (blue); metabolic rate – estimated metabolic rate instead of abundance for insect species (pink); plant biomass – estimated biomass instead of cover for plant species (green) (see Supplementary Text for details). The bottom left graphs show the posterior distribution for the case where no corrections are applied (reported in the main manuscript). Slope estimates are shown for combined land-use intensity (*LUI*) and for the single components of land-use intensity (mowing, grazing, fertilization). The estimates for the observed networks are in orange, and the estimates for the null models are in purple. Curves show probability densities of the posterior distributions, corresponding y-axes have been omitted for clarity; thin lines show the 95% highest density interval (HDI), bold lines show the 77.6% HDI, and points show the highest maximum a posteriori estimates. No overlap of 77.6% HDIs between the observation and null model indicates a significant difference on the 5% level.

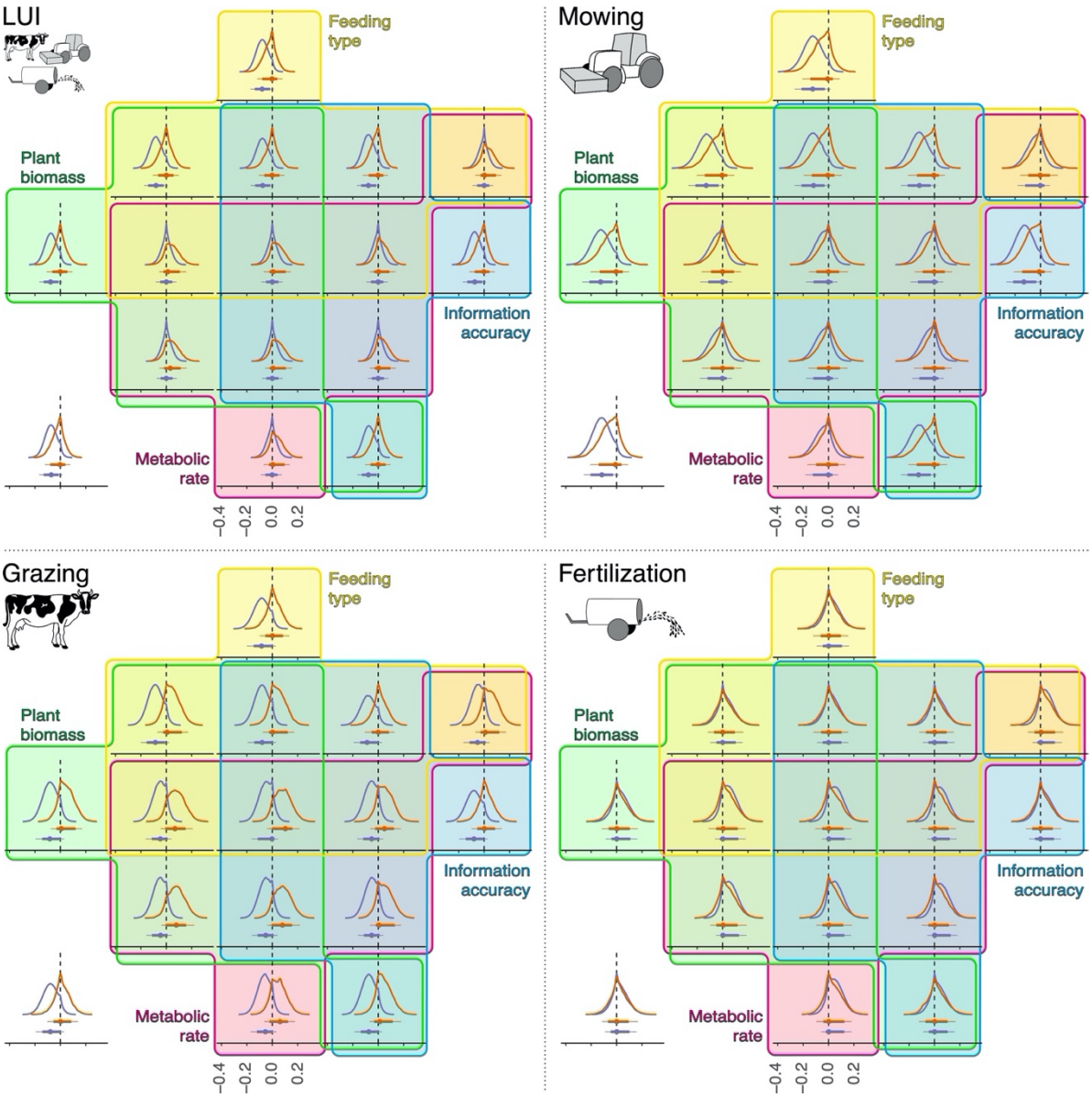

Fig. S9.

Grasslands: posterior distributions of slope estimates for models testing the effects of grassland land-use intensity on network nestedness. Each panel relies on a different correction method or on a combination of several methods as indicated by the overlaid colored shapes, each of which is representing a correction method: feeding type – down-weighing of omnivorous insect species (yellow); information accuracy – downweighing of interactions with less precise information on food plants (blue); metabolic rate – estimated metabolic rate instead of abundance for insect species (pink); plant biomass – estimated biomass instead of cover for plant species (green) (see Supplementary Text for details). The bottom left graphs show the posterior distribution for the case where no corrections are applied (reported in the main manuscript). Slope estimates are shown for combined land-use intensity (*LUI*) and for the single components of land-use intensity (mowing, grazing, fertilization). The estimates for the observed networks are in orange, and the estimates for the null models are in purple. Curves show probability densities of the posterior distributions, corresponding y-axes have been omitted for clarity; thin lines show the 95% highest density interval (HDI), bold lines show the 77.6% HDI, and points show the highest maximum a posteriori estimates. No overlap of 77.6% HDIs between the observation and null model indicates a significant difference on the 5% level.

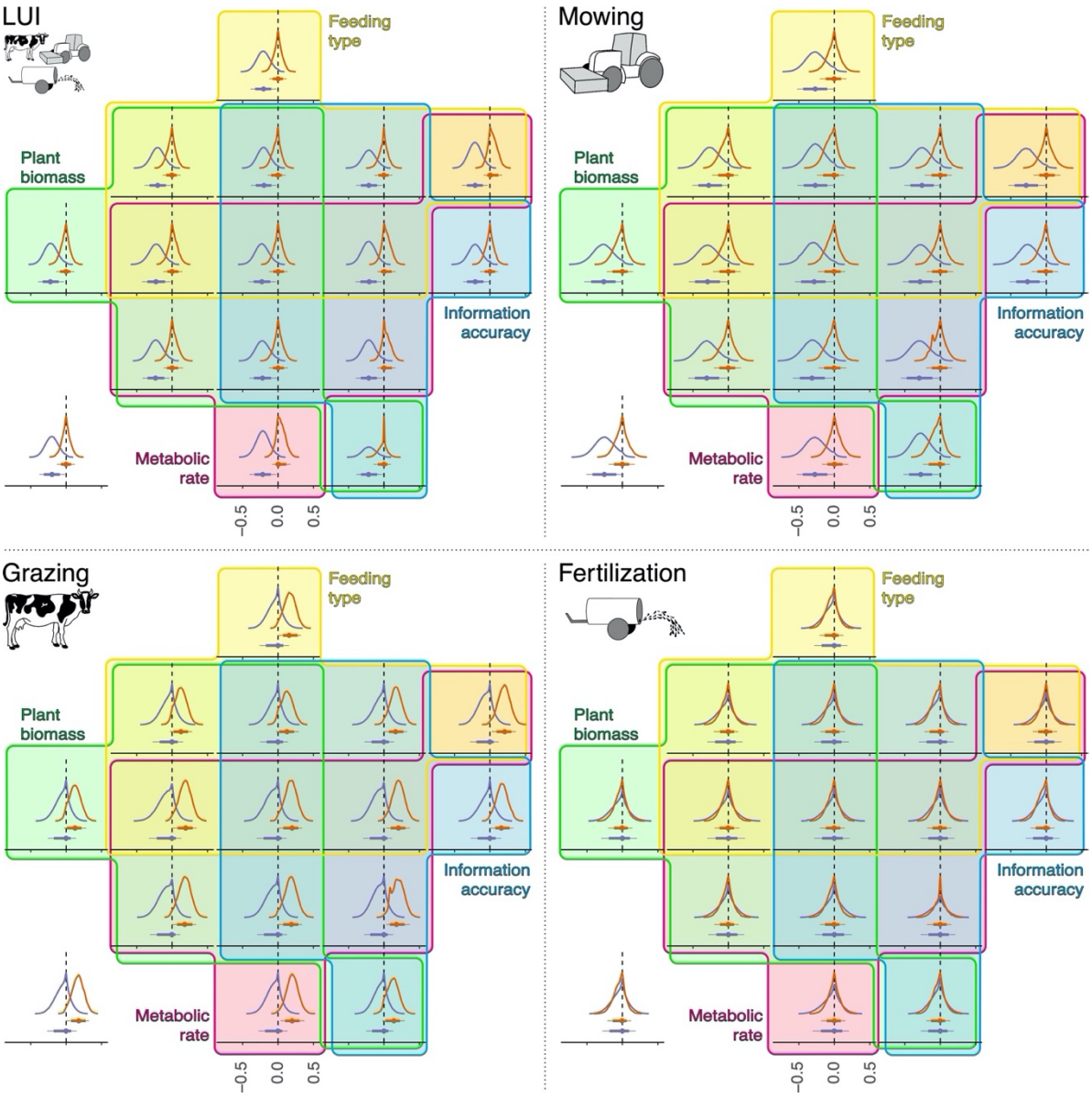

Fig. S10.

Grasslands: posterior distributions of slope estimates for models testing the effects of grassland land-use intensity on network robustness. Each panel relies on a different correction method or on a combination of several methods as indicated by the overlaid colored shapes, each of which is representing a correction method: feeding type – down-weighing of omnivorous insect species (yellow); information accuracy – downweighing of interactions with less precise information on food plants (blue); metabolic rate – estimated metabolic rate instead of abundance for insect species (pink); plant biomass – estimated biomass instead of cover for plant species (green) (see Supplementary Text for details). The bottom left graphs show the posterior distribution for the case where no corrections are applied (reported in the main manuscript). Slope estimates are shown for combined land-use intensity (*LUI*) and for the single components of land-use intensity (mowing, grazing, fertilization). The estimates for the observed networks are in orange, and the estimates for the null models are in purple. Curves show probability densities of the posterior distributions, corresponding y-axes have been omitted for clarity; thin lines show the 95% highest density interval (HDI), bold lines show the 77.6% HDI, and points show the highest maximum a posteriori estimates. No overlap of 77.6% HDIs between the observation and null model indicates a significant difference on the 5% level.

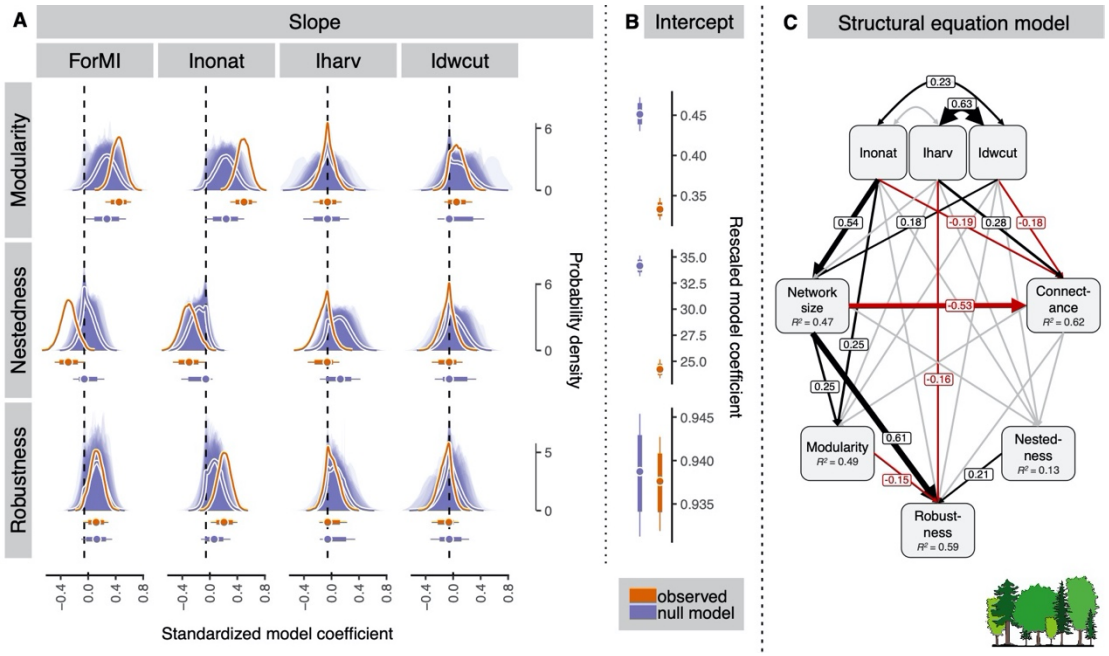

Fig. S11.

Forests: analyses for data of one year including herbivore data from forest canopies. Posterior distributions of (**A**) slope estimates and (**B**) intercept estimates for the fixed effects from hierarchical models testing the effects of land-use intensity on network metrics in observed networks (orange) and null model networks (purple), in which network size and connectance were kept constant. Slope estimates are shown for models on combined land-use intensity *(ForMI)* and for models on the single components of land-use intensity (*Inonat*: proportion of tree species that are not part of the natural community; *Iharv*: proportion of harvested wood volume; *Idwcut*: proportion of deadwood with saw cuts). Positive estimates indicate higher values at high land-use intensity. Intercept estimates correspond to overall means given that all variables were scaled. Intercepts were obtained from the model on the combined *ForMI* index. Values were rescaled to the original metric scale. Curves show probability densities of the posterior distributions; thin lines show the 95% highest density interval (HDI), bold lines show the 77.6% HDI, and points show the highest maximum a posteriori estimates. No overlap of 77.6% HDIs between the observation and null model indicates a significant difference on the 5% level. Shaded purple areas show the posterior distributions for single null-model realizations (n = 100). (**C**) Results from piecewise structural equation models testing the effects of land-use intensity components on basic network metrics (network size, connectance), modularity and nestedness, and their relationship with robustness. Numbers show standardized path coefficients for significant pathways. Network size was square-root transformed prior to analyses. Positive paths are in black, negative in red, and non-significant in grey. R^2 values (conditional) for all variables are provided within the boxes. Fisher's $C = 7.93$, $P = 0.019$.

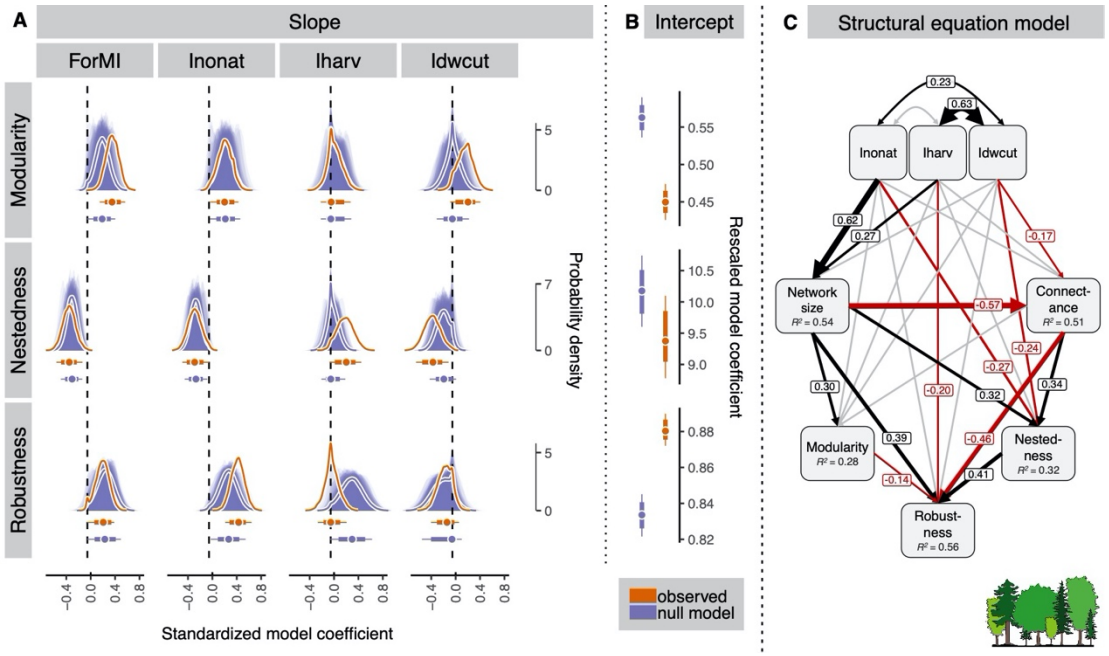

Fig. S12.

Forests: analyses for the case where imprecise interaction information was excluded from the interaction database (i.e., information higher than plant-family level). Posterior distributions of (**A**) slope estimates and (**B**) intercept estimates for the fixed effects from hierarchical models testing the effects of land-use intensity on network metrics in observed networks (orange) and null model networks (purple), in which network size and connectance were kept constant. Slope estimates are shown for models on combined land-use intensity *(ForMI)* and for models on the single components of land-use intensity (*Inonat*: proportion of tree species that are not part of the natural community; *Iharv*: proportion of harvested wood volume; *Idwcut*: proportion of deadwood with saw cuts). Positive estimates indicate higher values at high land-use intensity. Intercept estimates correspond to overall means given that all variables were scaled. Intercepts were obtained from the model on the combined *ForMI* index. Values were rescaled to the original metric scale. Curves show probability densities of the posterior distributions; thin lines show the 95% highest density interval (HDI), bold lines show the 77.6% HDI, and points show the highest maximum a posteriori estimates. No overlap of 77.6% HDIs between the observation and null model indicates a significant difference on the 5% level. Shaded purple areas show the posterior distributions for single null-model realizations (n = 100). (**C**) Results from piecewise structural equation models testing the effects of land-use intensity components on basic network metrics (network size, connectance), modularity and nestedness, and their relationship with robustness. Numbers show standardized path coefficients for significant pathways. Network size was square-root transformed prior to analyses. Positive paths are in black, negative in red, and non-significant in grey. R^2 values (conditional) for all variables are provided within the boxes. Fisher's $C = 0.29$, $P = 0.866$.

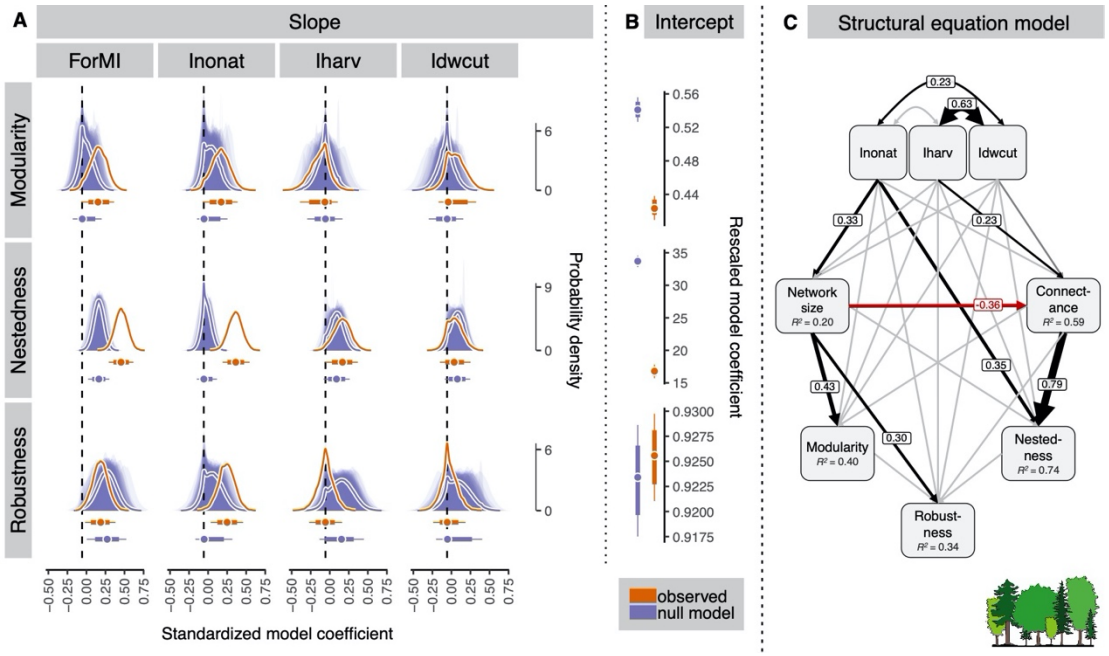

Fig. S13.

Forests: Analyses for the case where all plant species were added in very small quantities to all plots (i.e., no herbivores excluded because of missing food sources). Posterior distributions of (**A**) slope estimates and (**B**) intercept estimates for the fixed effects hierarchical models testing the effects of land-use intensity on network metrics in observed networks (orange) and null model networks (purple), in which network size and connectance were kept constant. Slope estimates are shown for models on combined land-use intensity *(ForMI)* and for models on the single components of land-use intensity (*Inonat*: proportion of tree species that are not part of the natural community; *Iharv*: proportion of harvested wood volume; *Idwcut*: proportion of deadwood with saw cuts). Positive estimates indicate higher values at high land-use intensity. Intercept estimates correspond to overall means given that all variables were scaled. Intercepts were obtained from the model on the combined *ForMI* index. Values were rescaled to the original metric scale. Curves show probability densities of the posterior distributions; thin lines show the 95% highest density interval (HDI), bold lines show the 77.6% HDI, and points show the highest maximum a posteriori estimates. No overlap of 77.6% HDIs between the observation and null model indicates a significant difference on the 5% level. Shaded purple areas show the posterior distributions for single null-model realizations (n = 100). (**C**) Results from piecewise structural equation models testing the effects of land-use intensity components on basic network metrics (network size, connectance), modularity and nestedness, and their relationship with robustness. Numbers show standardized path coefficients for significant pathways. Network size was square-root transformed prior to analyses. Positive paths are in black, negative in red, and non-significant in grey. R^2 values (conditional) for all variables are provided within the boxes. Fisher's $C = 13.50$, $P = 0.001$.

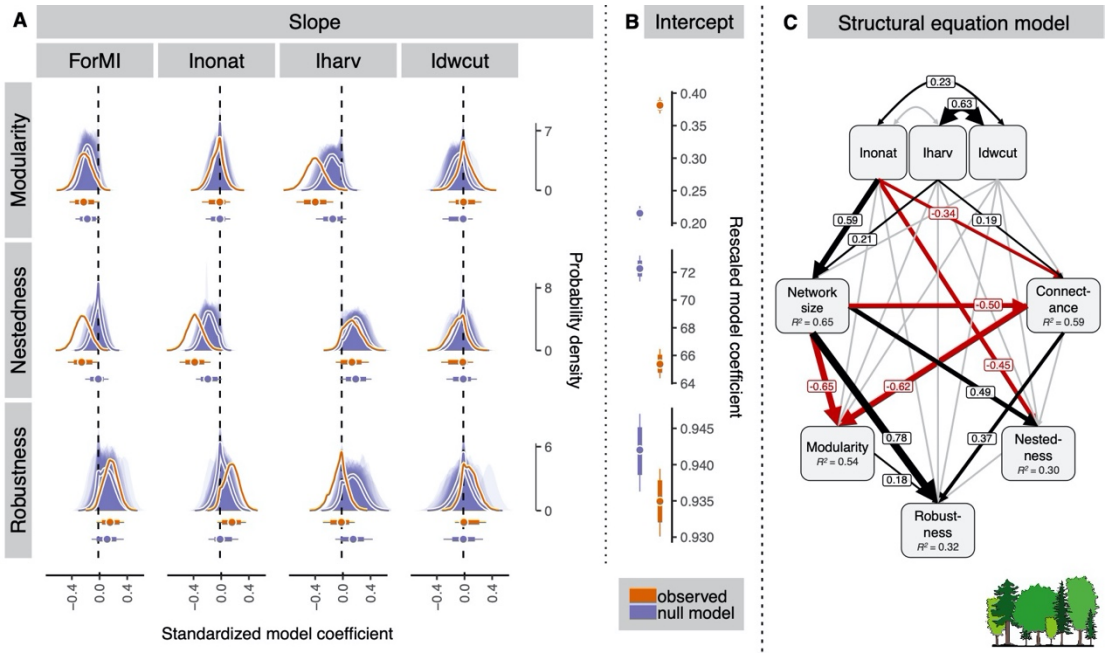

Fig. S14.

Forests: Analyses for the case where interaction strength was not considered (i.e., presence–absence networks). Posterior distributions of (**A**) slope estimates and (**B**) intercept estimates for the fixed effects from hierarchical models testing the effects of land-use intensity on network metrics in observed networks (orange) and null model networks (purple), in which network size and connectance were kept constant. Slope estimates are shown for models on combined land-use intensity *(ForMI)* and for models on the single components of land-use intensity (*Inonat*: proportion of tree species that are not part of the natural community; *Iharv*: proportion of harvested wood volume; *Idwcut*: proportion of deadwood with saw cuts). Positive estimates indicate higher values at high land-use intensity. Intercept estimates correspond to overall means given that all variables were scaled. Intercepts were obtained from the model on the combined *ForMI* index. Values were rescaled to the original metric scale. Curves show probability densities of the posterior distributions; thin lines show the 95% highest density interval (HDI), bold lines show the 77.6% HDI, and points show the highest maximum a posteriori estimates. No overlap of 77.6% HDIs between the observation and null model indicates a significant difference on the 5% level. Shaded purple areas show the posterior distributions for single null-model realizations (n = 100). (**C**) Results from piecewise structural equation models testing the effects of land-use intensity components on basic network metrics (network size, connectance), modularity and nestedness, and their relationship with robustness. Numbers show standardized path coefficients for significant pathways. Network size was square-root transformed prior to analyses. Positive paths are in black, negative in red, and non-significant in grey. R^2 values (conditional) for all variables are provided within the boxes. Fisher's $C = 14.78$, $P = 0.001$.

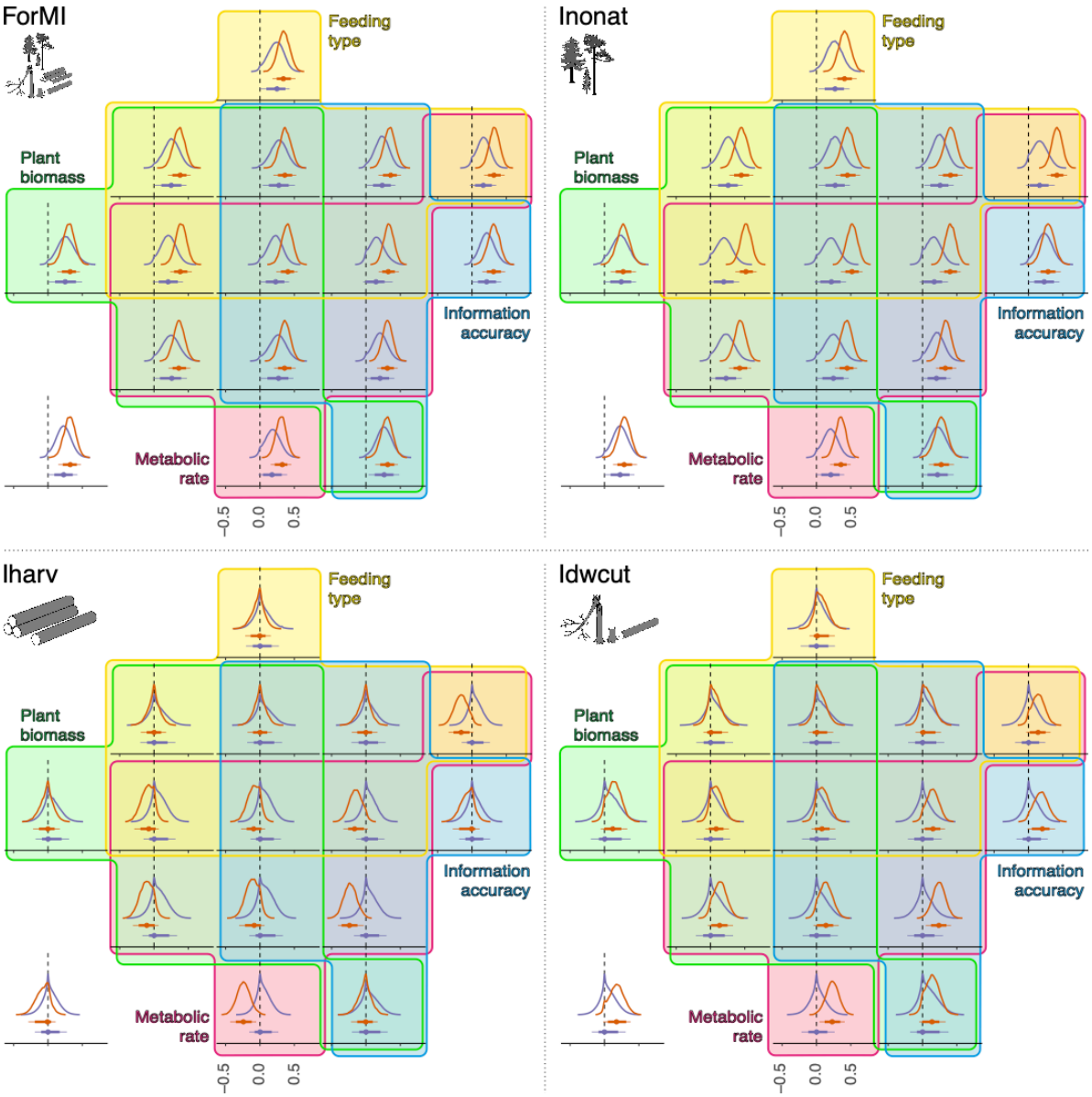

Fig. S15.

Forests: posterior distributions of slope estimates for models testing the effects of forest land-use intensity on network modularity. Each panel relies on a different correction method or on a combination of several methods as indicated by the overlaid colored shapes, each of which is representing a correction method: feeding type – downweighing of omnivorous insect species (yellow); information accuracy – downweighing of interactions with less precise information on food plants (blue); metabolic rate – estimated metabolic rate instead of abundance for insect species (pink); plant biomass – estimated biomass instead of cover for plant species (green) (see Supplementary Text for details). The bottom left graphs show the posterior distribution for the case where no corrections are applied (reported in the main manuscript). Slope estimates are shown for combined land-use intensity (*ForMI*) and for the single components of land-use intensity (*Inonat*: proportion of tree species that are not part of the natural community; *Iharv*: proportion of harvested wood volume; *Idwcut*: proportion of deadwood with saw cuts). The estimates for the observed networks are in orange, and the estimates for the null models are in purple. Curves show probability densities of the posterior distributions, corresponding y-axes have been omitted for clarity; thin lines show the 95% highest density interval (HDI), bold lines show the 77.6% HDI, and points show the highest maximum a posteriori estimates. No overlap of 77.6% HDIs between the observation and null model indicates a significant difference on the 5% level.

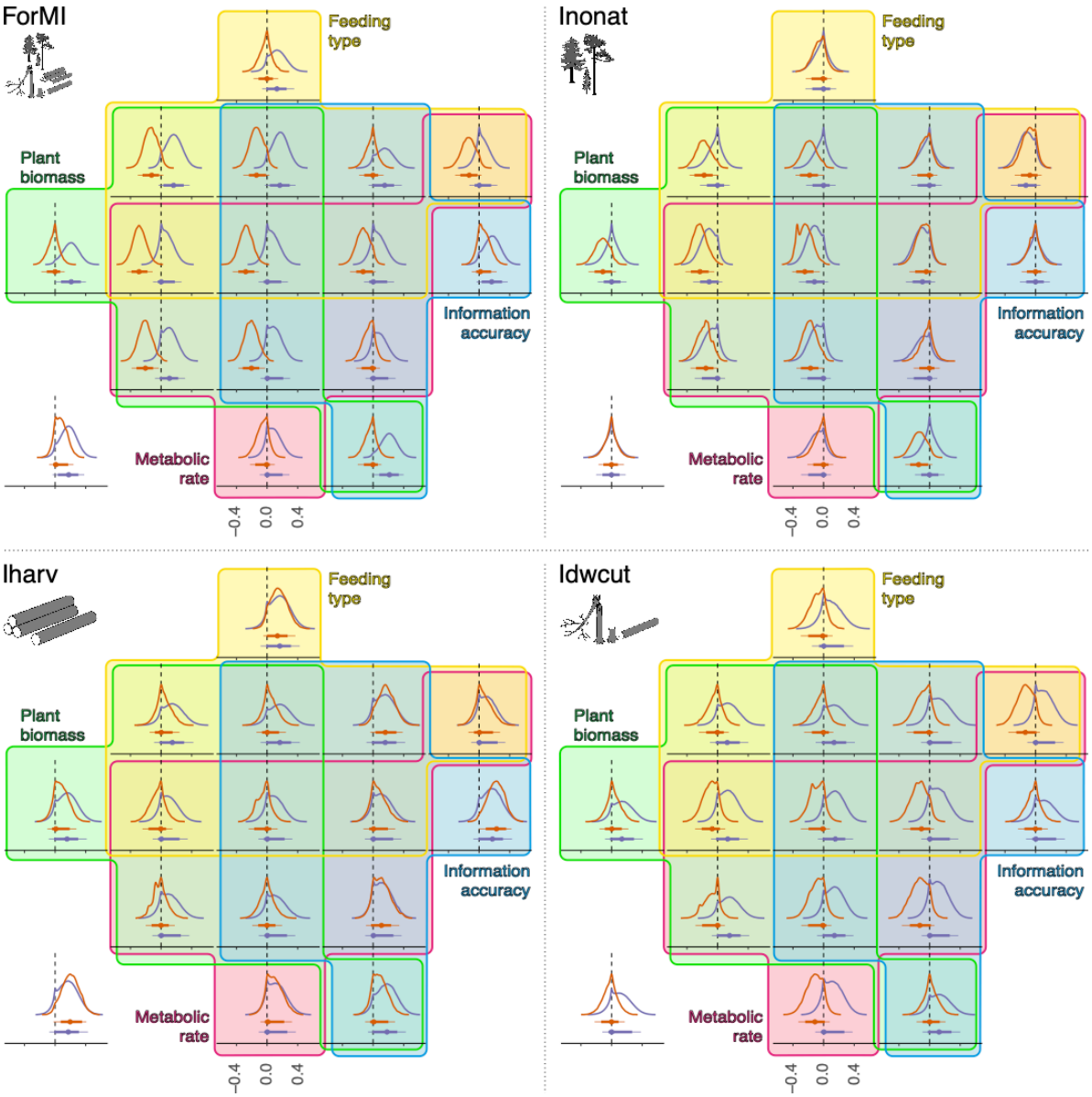

Fig. S16.

Forests: posterior distributions of slope estimates for models testing the effects of forest land-use intensity on network nestedness. Each panel relies on a different correction method or on a combination of several methods as indicated by the overlaid colored shapes, each of which is representing a correction method: feeding type – downweighing of omnivorous insect species (yellow); information accuracy – downweighing of interactions with less precise information on food plants (blue); metabolic rate – estimated metabolic rate instead of abundance for insect species (pink); plant biomass – estimated biomass instead of cover for plant species (green) (see Supplementary Text for details). The bottom left graphs show the posterior distribution for the case where no corrections are applied (reported in the main manuscript). Slope estimates are shown for combined land-use intensity (*ForMI*) and for the single components of land-use intensity (*Inonat*: proportion of tree species that are not part of the natural community; *Iharv*: proportion of harvested wood volume; *Idwcut*: proportion of deadwood with saw cuts). The estimates for the observed networks are in orange, and the estimates for the null models are in purple. Curves show probability densities of the posterior distributions, corresponding y-axes have been omitted for clarity; thin lines show the 95% highest density interval (HDI), bold lines show the 77.6% HDI, and points show the highest maximum a posteriori estimates. No overlap of 77.6% HDIs between the observation and null model indicates a significant difference on the 5% level.

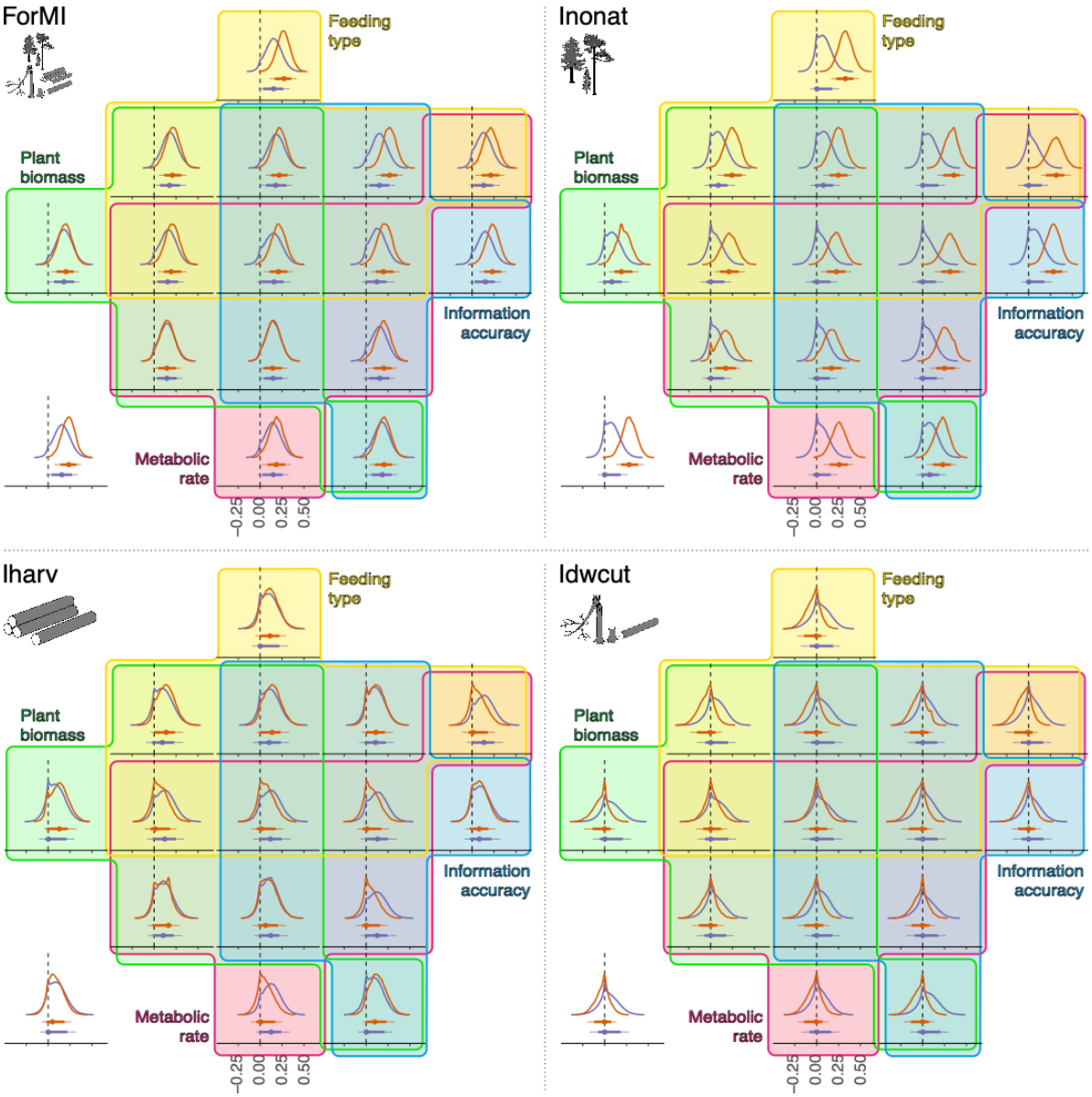

Fig. S17.

Forests: posterior distributions of slope estimates for models testing the effects of forest land-use intensity on network robustness. Each panel relies on a different correction method or on a combination of several methods as indicated by the overlaid colored shapes, each of which is representing a correction method: feeding type – downweighing of omnivorous insect species (yellow); information accuracy – downweighing of interactions with less precise information on food plants (blue); metabolic rate – estimated metabolic rate instead of abundance for insect species (pink); plant biomass – estimated biomass instead of cover for plant species (green) (see Supplementary Text for details). The bottom left graphs show the posterior distribution for the case where no corrections are applied (reported in the main manuscript). Slope estimates are shown for combined land-use intensity (*ForMI*) and for the single components of land-use intensity (*Inonat*: proportion of tree species that are not part of the natural community; *Iharv*: proportion of harvested wood volume; *Idwcut*: proportion of deadwood with saw cuts). The estimates for the observed networks are in orange, and the estimates for the null models are in purple. Curves show probability densities of the posterior distributions, corresponding y-axes have been omitted for clarity; thin lines show the 95% highest density interval (HDI), bold lines show the 77.6% HDI, and points show the highest maximum a posteriori estimates. No overlap of 77.6% HDIs between the observation and null model indicates a significant difference on the 5% level.

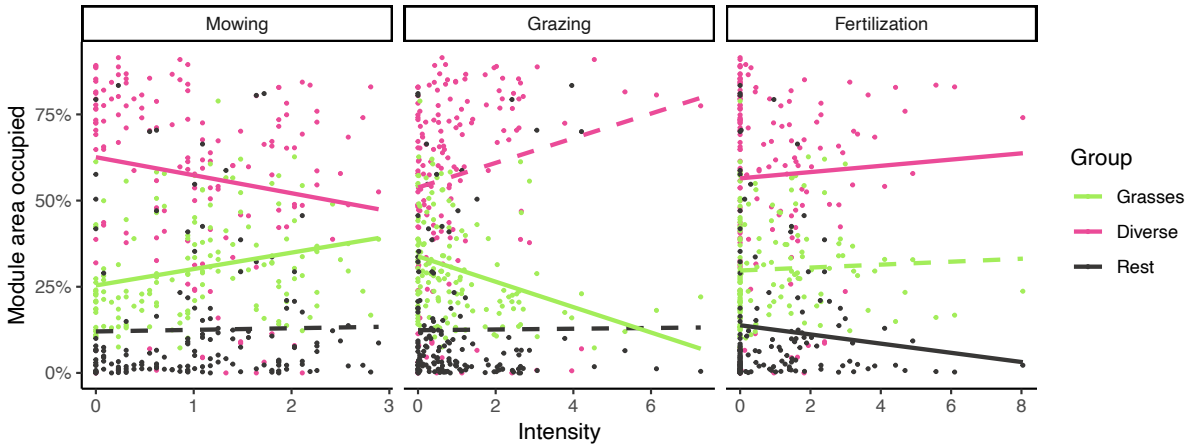

Fig. S18.

Percentage of the module area occupied by modules belonging to three different groups based on the plant species composition of the modules, shown along the gradient of intensity of mowing, grazing and fertilization. If more than 50% of plant species are of one plant order, a module is categorized as *Grasses* (for Poales) or *Rest* (other plant orders). If plants cannot be categorized to a main plant order, a module is categorized as *Diverse*. Each point denotes a plot and module category. Lines show separate linear models. Linear mixed effects models on the combined effect of intensity and frequency of mowing, grazing and fertilization show a significant positive effect of mowing (t = 2.024, df = 145.9, P = 0.0448) and a significant negative effect of grazing (t = -2.828, df = 146.0, P = 0.00534) on the proportion of *Grasses* modules (Satterthwaite's method in R package *lmer*).

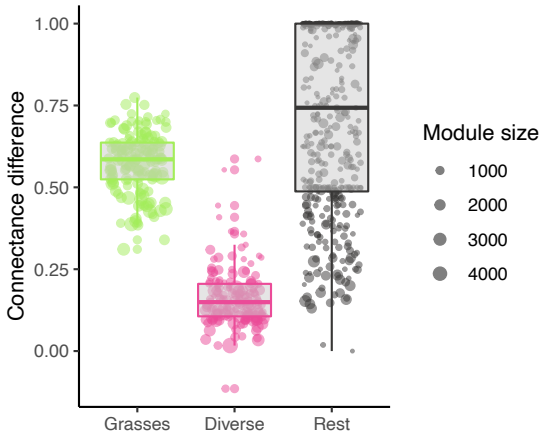

Fig. S19.

Difference between connectance within a module and connectance outside of this module (i.e., across all other plant species in the plot). A difference of 1 indicates complete connectance within a module and no interactions of the herbivores with plants outside of the module. Values around 0 indicate similar connectance within and outside a module. If more than 50% of plant species are of one plant order, a module is categorized as *Grasses* (for Poales) or *Rest* (other plant orders). If plants cannot be categorized to a main plant order, a module is categorized as *Diverse*. Each point denotes a module in a plot, with point size indicating module size (i.e., number of plants times number of herbivores). The boxplots summarize the distribution of values. Components are mid line (median), box edges (first and third quartiles), and whiskers (extend to the lowest and highest observed values that lie within 1.5 times the interquartile distance).

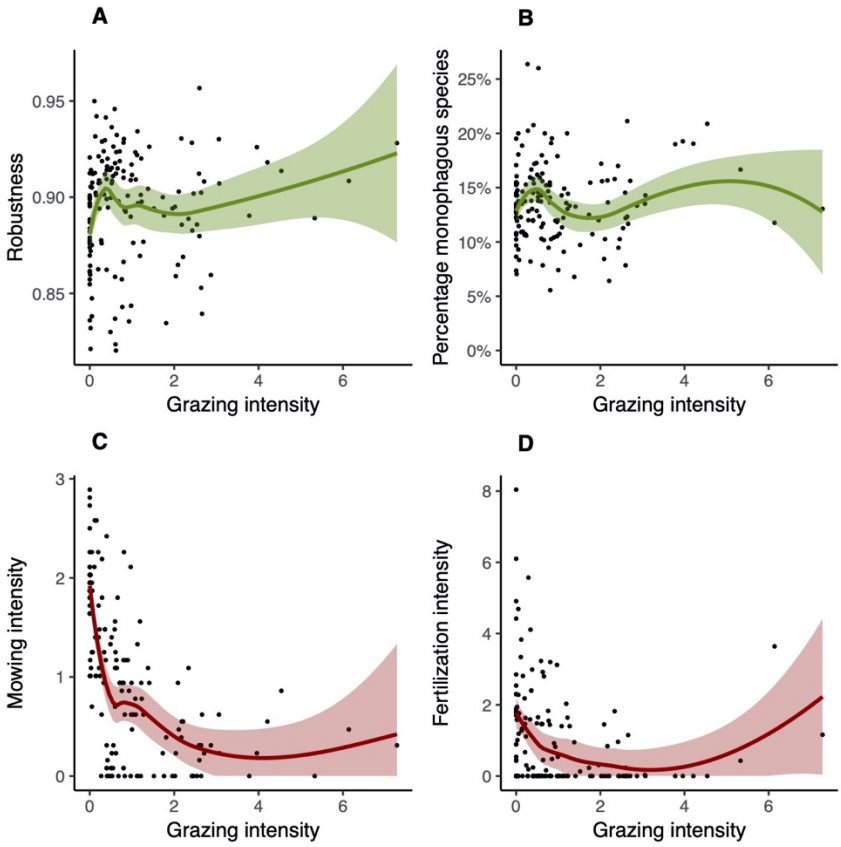

Fig. S20.

(**A**) Robustness and (**B**) percentage of species categorized as monophagous (i.e., feeding on plant species of one genus only) (**C**) mowing intensity and (**D**) fertilization intensity along the gradient of grazing intensity. Points represent plots (n = 150), and lines and shading show a local polynomial regression line with 95% confidence bands.

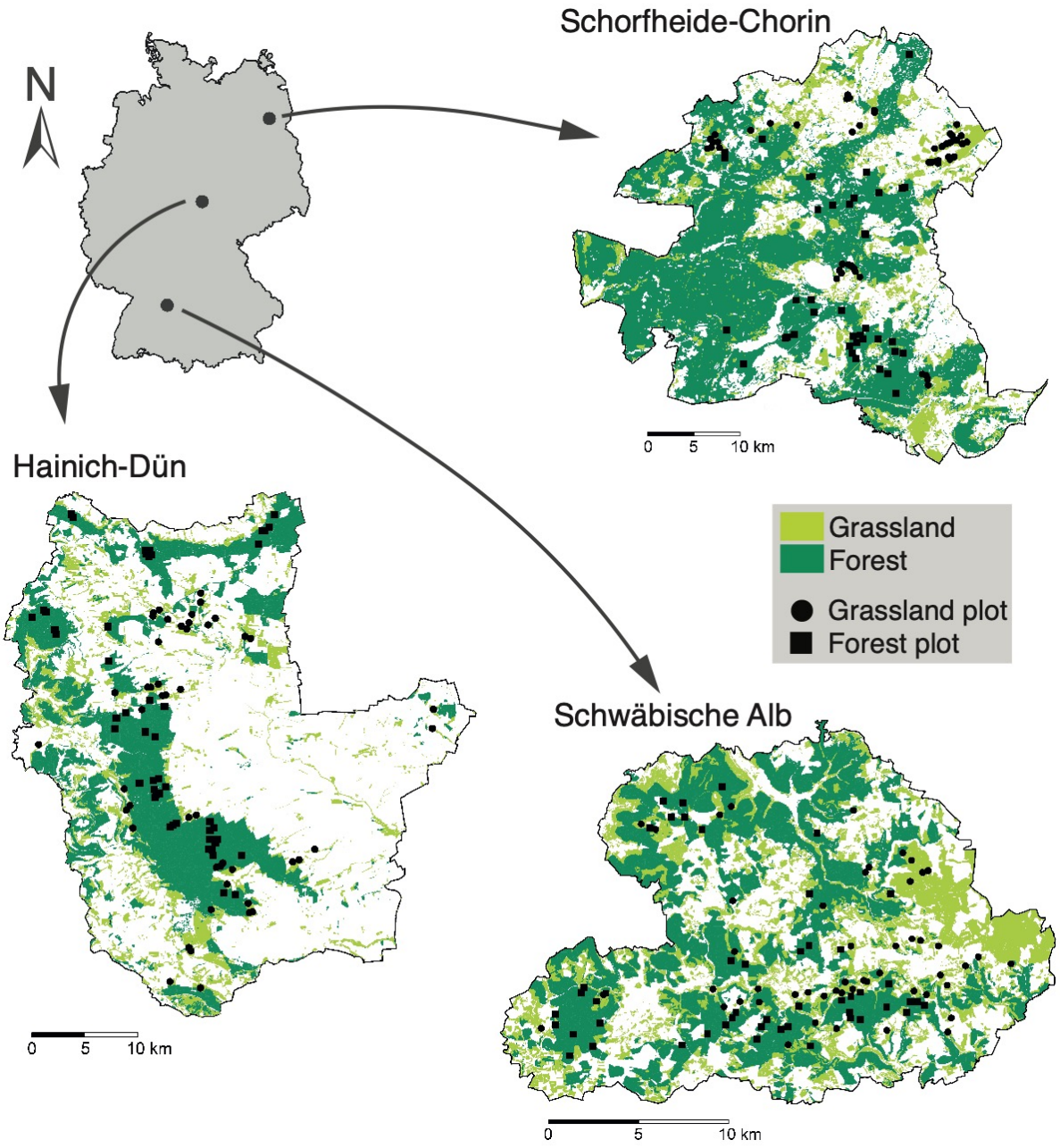

Fig. S21.

Maps of the three study regions (Schorfheide-Chorin, Hainich-Dün, Schwäbische Alb). The panel on the top left shows the location of the three regions within Germany, the detail maps of all regions show grassland and forest ecosystems. The position of all plots used for the analyses is shown (n = 289). The maps were produced in collaboration with the local management teams of the Biodiversity Exploratories.

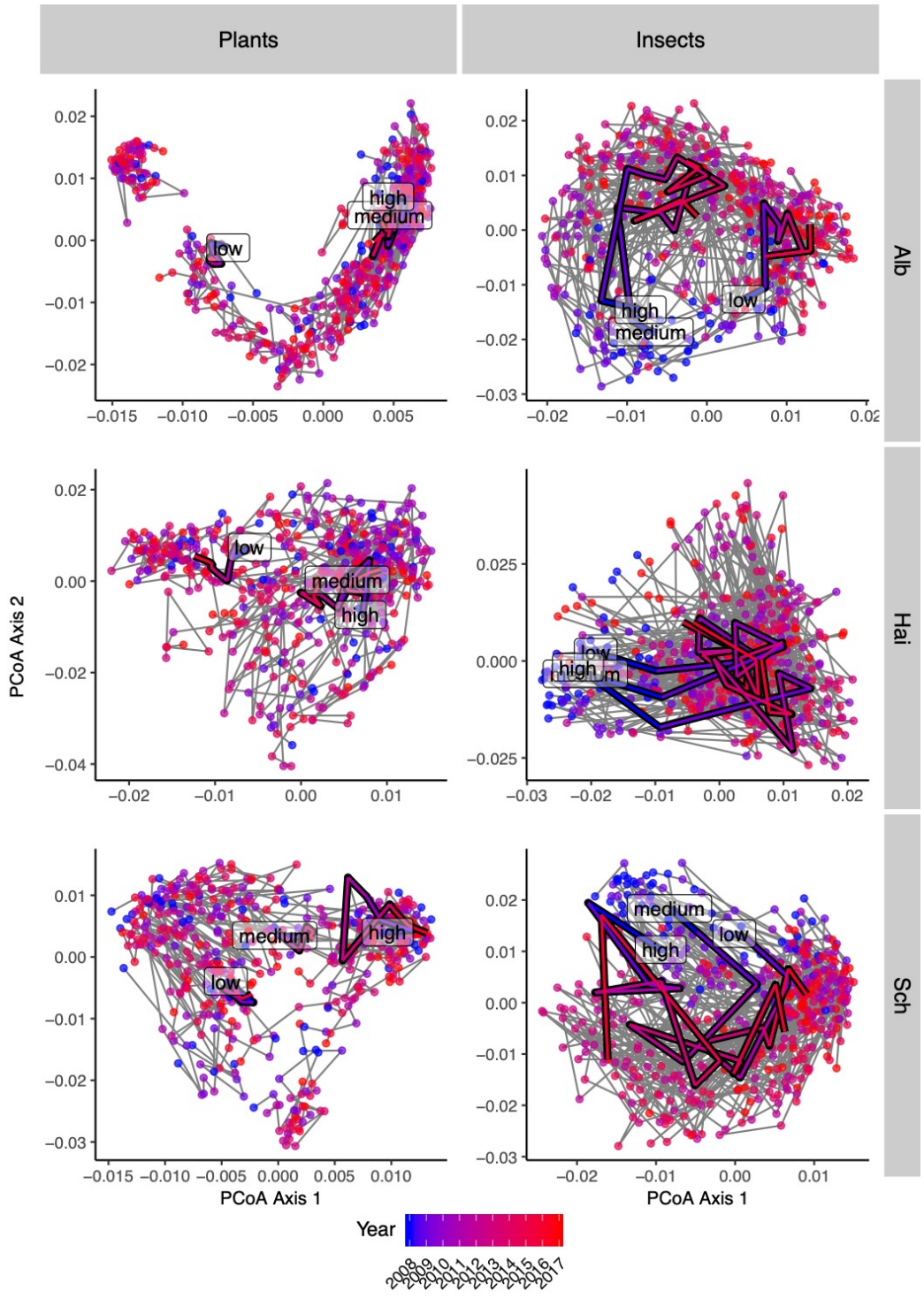

Fig. S22.

Grasslands: Community composition of plants (left) and herbivorous insects (right) for each plot and sampling year expressed in two axes from principal coordinates analysis (PCoA) based on Bray-Curtis distances between communities. Separate analyses were conducted for the three study regions. Each point shows one plot and year, colors indicate the year of sampling and grey lines connect samplings of the same plot. Bold lines connect mean values for each sampling year for three groups of plots, separated by land-use intensity (*LUI*) into three categories (low, medium, high).

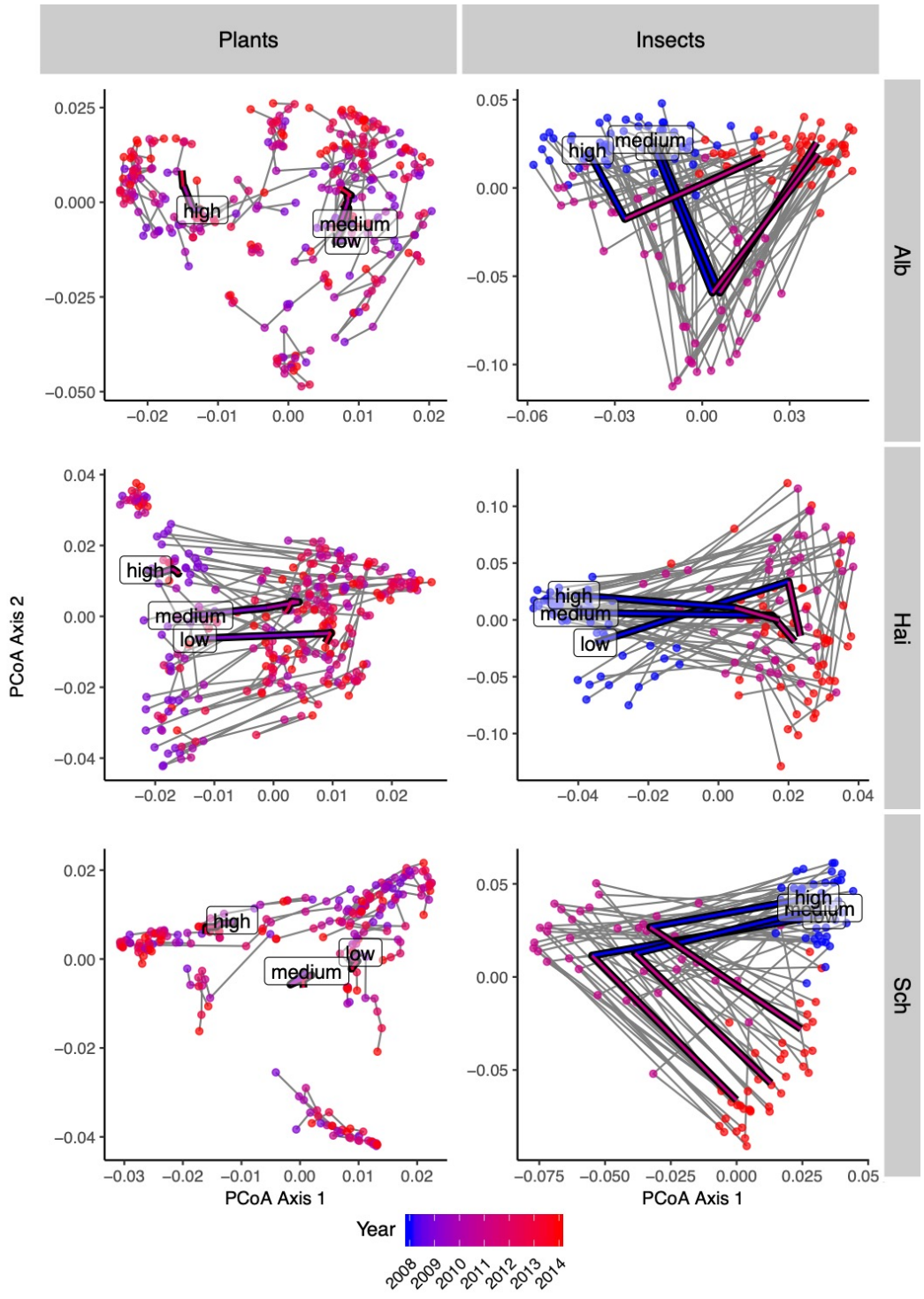

Fig. S23.

Forests: Community composition of plants (left) and herbivorous insects (right) for each plot and sampling year expressed in two axes from principal coordinates analysis (PCoA) based on Bray-Curtis distances between communities. Separate analyses were conducted for the three study regions. Each point shows one plot and year, colors indicate the year of sampling and grey lines connect samplings of the same plot. Bold lines connect mean values for each sampling year for three groups of plots, separated by land-use intensity (*ForMI*) into three categories (low, medium, high). Plant data only includes annual vegetation surveys but not regeneration and tree inventories.

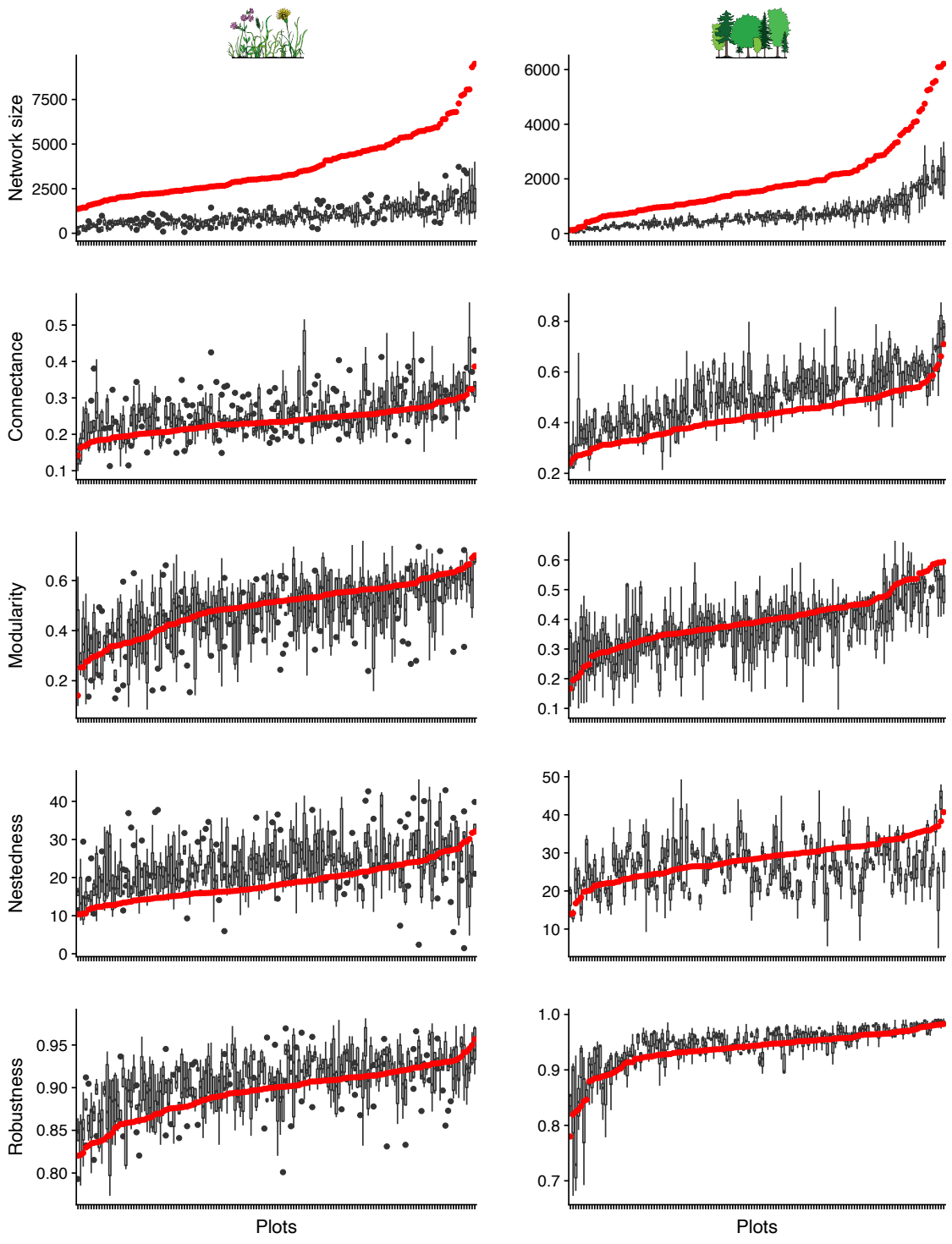

Fig. S24.

Network metrics for temporally resolved networks in grasslands (left) and forests (right). In grasslands, two consecutive years were pooled, resulting in a total of five timesteps. In forests, the three sampling years were analyzed separately. For each metric and system, the values are shown arranged by plot, sorted by the value determined for the pooled data. Values for temporally resolved data are shown with boxplots, values for the pooled data are shown with the red dots.

Table S1.

Sampling numbers (numbers of species/genera and number of individuals) for all insect groups.

		Sweep netting (grasslands)							Flight-interception traps (forests)						
		Juv.	No ID	No spec.	No herb.	No info.	No vasc.	Remain	Juv.	No ID	No spec.	No herb.	No info.	No vasc.	Remain
Auchenorr.	Genus/ Species	–	–	4	0	1	0	161	–	–	4 (+3)	0 (+0)	0 (+0)	0 (+0)	65 (+14)
	Abund.	18,488	56	6	0	6	0	106,983	389 (+106)	43 (+78)	4 (+4)	0 (+0)	0 (+0)	0 (+0)	768 (+677)
Heteroptera	Genus/ Species	–	–	2	21	0	2	180	–	–	1 (+2)	46 (+7)	0 (+0)	1 (+1)	147 (+27)
	Abund.	74,538	280	2	863	0	3	45,470	1,074 (+243)	94 (+82)	1 (+2)	745 (+568)	0 (+0)	1 (+1)	3,871 (+5,942)
Coleoptera	Genus/ Species	–	–	1	318	15	2	406	–	–	0 (+0)	1,150 (+61)	27 (+1)	2 (+1)	334 (+31)
	Abund.	–	8	6	7,068	93	3	28,932	–	32 (+18)	0 (+0)	74,108 (+10,781)	2,011 (+181)	5 (+1)	44,275 (+9,854)
Orthoptera	Genus/ Species	–	–	0	1	0	0	27	–	–	0 (+0)	1 (+0)	0 (+0)	0 (+0)	6 (+1)
	Abund.	6,396	169	0	1	0	0	3,143	6 (+29)	0 (+0)	0 (+0)	62 (+164)	0 (+0)	0 (+0)	20 (+6)

For flight-interception traps, numbers in brackets show numbers from additional samples taken in forest canopies only in 2008. Numbers of species/genera show additional species/genera.

Juv.: Number of juvenile individuals sampled. Only recorded for hemimetabolic insect groups. Juveniles were excluded from further analyses.

No ID: Individuals not identified to the genus or species level. These individuals were excluded from further analyses.

No spec.: Genus-level specimens that could not be assigned to the species level. These individuals were excluded from further analyses.

No herb.: Species without a herbivorous diet. These individuals were excluded from further analyses.

No info.: Herbivorous species for which no information on food plants could be found in the literature. These individuals were excluded from further analyses.

No vasc.: Herbivorous species only feeding on non-vascular plants (bryophytes, algae, lichens). These individuals were excluded from further analyses.

Remain: Remaining number of species/individuals, which were used for analyses.

Auchenorr.: Auchenorrhyncha

Table S2.

Detailed results from structural equation modeling for the relations among different network metrics without including land-use intensity. Standardized estimates for all pathways linking response and predictor variables are reported and significances indicated (*** : $P \leq 0.001$, ** : $P \leq 0.01$, * : $P \leq 0.05$). Conditional R^2 values are given for all response variables. Different analyses were run for the two ecosystems (grasslands, forests) and different sensitivity scenarios were used. Fisher's C values and significance for all structural equation models are reported in the sensitivity scenario column. Note that network size was square-root transformed.

	Sensitivity scenario	Response	Predictor				R^2
			Network size	Connectance	Modularity	Nestedness	
Grasslands	– ($C = 0.04$)	Connectance	-0.16***	–	–	–	0.19
		Modularity	0.21	-0.23	–	–	0.05
		Nestedness	0.07	-0.14	–	–	0.63
		Robustness	0.008***	0.009	0.000	0.024***	0.48
	no impr. ($C = 5.95$)	Connectance	-0.53***	–	–	–	0.51
		Modularity	0.12	-0.24	–	–	0.08
		Nestedness	0.02	0.46***	–	–	0.27
		Robustness	0.013***	-0.010	0.003	0.022***	0.41
	all plants ($C = 2.41$)	Connectance	-0.13***	–	–	–	0.50
		Modularity	0.29**	-0.24	–	–	0.12
		Nestedness	0.04	1.04***	–	–	0.71
		Robustness	0.003	-0.004	-0.000	0.008	0.05
	pres.-abs. ($C = 2.88$)	Connectance	-0.16***	–	–	–	0.19
		Modularity	0.01	-1.06***	–	–	0.32
		Nestedness	0.21***	1.10***	–	–	0.61
		Robustness	-0.011***	-0.028***	0.014***	0.039***	0.55
Forests	– ($C = 0.39$)	Connectance	-0.60***	–	–	–	0.61
		Modularity	0.38***	-0.15	–	–	0.25
		Nestedness	0.31***	0.19*	–	–	0.10
		Robustness	0.021***	-0.001	-0.010***	0.017***	0.54
	no impr. ($C = 0.01$)	Connectance	-1.32***	–	–	–	0.49
		Modularity	0.55**	-0.16	–	–	0.26
		Nestedness	0.33	0.38***	–	–	0.16
		Robustness	0.036***	-0.018***	-0.008*	0.018***	0.52
	all plants ($C = 12.22$**)	Connectance	-0.45***	–	–	–	0.55
		Modularity	0.52***	-0.08	–	–	0.35
		Nestedness	0.29**	0.93***	–	–	0.68
		Robustness	0.013***	0.002	-0.002	0.003	0.33
	pres.-abs. ($C = 9.25$*)	Connectance	-0.60***	–	–	–	0.61
		Modularity	-0.94***	-0.94***	–	–	0.53
		Nestedness	0.27**	0.38***	–	–	0.17
		Robustness	0.025***	0.015***	0.006*	0.000	0.31

Sensitivity scenarios: –: data as presented in the main manuscript; *no impr.*: imprecise interaction information was excluded from the interaction data base (i.e., information higher than plant-family level); *all plants*: all plant species were added in very small quantities to all plots (i.e., no herbivores excluded because of missing food sources); *pres.-abs.*: interaction strength was not considered (i.e., presence–absence networks)

Table S3.

Summarized path coefficients from structural equation modelling for the effects of land-use intensity on network robustness. Two different models are shown (grasslands, forests) and effects are shown for the different land-use components. Indirect pathways are split into three categories: through basic network metrics (network size, connectance), modularity and nestedness. Total path coefficients show the sum of all indirect and direct pathways.

Model	Driver	Indirect			Direct	**Total**
		Basic metrics	Modularity	Nestedness		
Grassland	Mowing	-0.14	0.00	-0.04	0.19	**0.01**
	Grazing	-0.05	-0.02	0.01	0.26	**0.19**
	Fertilization	-0.03	-0.02	0.02	-0.04	**-0.06**
Forest	*Inonat*	0.29	-0.07	-0.01	0.08	**0.30**
	Iharv	0.12	0.02	0.09	-0.10	**0.13**
	Idwcut	0.04	-0.05	-0.01	-0.03	**-0.05**

Significant and non-significant pathways are included in this summary.

Positive coefficients are in black, negative coefficients in red.

Inonat: proportion of tree species that are not part of the natural community.

Iharv: proportion of harvested wood volume.

Idwcut: proportion of deadwood with saw cuts.

Table S4.

Overview of literature sources used to compile the interaction database.

Taxon	Sources
Auchenorrhyncha	refs. (*77*, *79*)
Heteroptera	refs. (*80–97*)
Coleoptera	refs. (*82*, *98–110*)
Orthoptera	refs. (*111–113*)

Table S5.

Prior distributions for hierarchical model parameters.

Parameter	Prior distribution
σ_α	$\sigma_\alpha \sim \text{Cauchy}(0, 1) \in [0, 100]$
σ_{β_j}	$\sigma_{\beta_j} \sim \text{Cauchy}(0, 2.5) \in [0, 100]$
σ_y	$\sigma_y \sim \text{Cauchy}(0, 25) \in [0, 100]$

REFERENCES AND NOTES

1. H. M. Pereira, P. W. Leadley, V. Proença, R. Alkemade, J. P. W. Scharlemann, J. F. Fernandez-Manjarrés, M. B. Araújo, P. Balvanera, R. Biggs, W. W. L. Cheung, L. Chini, H. D. Cooper, E. L. Gilman, S. Guénette, G. C. Hurtt, H. P. Huntington, G. M. Mace, T. Oberdorff, C. Revenga, P. Rodrigues, R. J. Scholes, U. R. Sumaila, M. Walpole, Scenarios for global biodiversity in the 21st century. *Science* **330**, 1496–1501 (2010).

2. O. E. Sala, F. S. Chapin III, J. J. Armesto, E. Berlow, J. Bloomfield, R. Dirzo, E. Huber-Sannwald, L. F. Huenneke, R. B. Jackson, A. Kinzig, R. Leemans, D. M. Lodge, H. A. Mooney, M. Oesterheld, N. L. Poff, M. T. Sykes, B. H. Walker, M. Walker, D. H. Wall, Global biodiversity scenarios for the year 2100. *Science* **287**, 1770–1774 (2000).

3. J. C. Habel, J. Dengler, M. Janišová, P. Török, C. Wellstein, M. Wiezik, European grassland ecosystems: Threatened hotspots of biodiversity. *Biodivers. Conserv.* **22**, 2131–2138 (2013).

4. J. Bauhus, K. J. Puettmann, C. Kühne, in *Managing Forests as Complex Adaptive Systems: Building Resilience to the Challenge of Global Change*, C. Messier, K. J. Puettmann, K. D. Coates, Eds. (The Earthscan Forest Library, Routledge, 2013), pp. 187–213.

5. M. M. Gossner, T. Lachat, J. Brunet, G. Isacsson, C. Bouget, H. Brustel, R. Brandl, W. W. Weisser, J. Müller, Current near-to-nature forest management effects on functional trait composition of saproxylic beetles in beech forests. *Conserv. Biol.* **27**, 605–614 (2013).

6. A. J. A. M. Temme, P. H. Verburg, Mapping and modelling of changes in agricultural intensity in Europe. *Agric. Ecosyst. Environ.* **140**, 46–56 (2011).

7. E. Allan, P. Manning, F. Alt, J. Binkenstein, S. Blaser, N. Blüthgen, S. Böhm, F. Grassein, N. Hölzel, V. H. Klaus, T. Kleinebecker, E. K. Morris, Y. Oelmann, D. Prati, S. C. Renner, M. C. Rillig, M. Schaefer, M. Schloter, B. Schmitt, I. Schöning, M. Schrumpf, E. Solly, E. Sorkau, J. Steckel, I. Steffen-Dewenter, B. Stempfhuber, M. Tschapka, C. N. Weiner, W. W. Weisser, M. Werner, C. Westphal, W. Wilcke, M. Fischer, Land use intensification alters ecosystem multifunctionality via loss of biodiversity and changes to functional composition. *Ecol. Lett.* **18**, 834–843 (2015).

8. S. A. Socher, D. Prati, S. Boch, J. Müller, V. H. Klaus, N. Hölzel, M. Fischer, Direct and productivity-mediated indirect effects of fertilization, mowing and grazing on grassland species richness. *J. Ecol.* **100**, 1391–1399 (2012).

9. A. Chaudhary, Z. Burivalova, L. P. Koh, S. Hellweg, Impact of forest management on species richness: Global meta-analysis and economic trade-offs. *Sci. Rep.* **6**, 23954 (2016).

10. C. Penone, E. Allan, S. Soliveres, M. R. Felipe-Lucia, M. M. Gossner, S. Seibold, N. K. Simons, P. Schall, F. van der Plas, P. Manning, R. D. Manzanedo, S. Boch, D. Prati, C. Ammer, J. Bauhus, F. Buscot, M. Ehbrecht, K. Goldmann, K. Jung, J. Müller, J. C. Müller, R. Pena, A. Polle, S. C. Renner, L. Ruess, I. Schönig, M. Schrumpf, E. F. Solly, M. Tschapka, W. W. Weisser, T. Wubet, M. Fischer, Specialisation and diversity of multiple trophic groups are promoted by different forest features. *Ecol. Lett.* **22**, 170–180 (2019).

11. F. Neff, N. Blüthgen, M. N. Chisté, N. K. Simons, J. Steckel, W. W. Weisser, C. Westphal, L. Pellissier, M. M. Gossner, Cross-scale effects of land use on the functional composition of herbivorous insect communities. *Landsc. Ecol.* **34**, 2001–2015 (2019).

12. S. Soliveres, F. van Der Plas, P. Manning, D. Prati, M. M. Gossner, S. C. Renner, F. Alt, H. Arndt, V. Baumgartner, J. Binkenstein, K. Birkhofer, S. Blaser, N. Blüthgen, S. Boch, S. Böhm, C. Börschig, F. Buscot, T. Diekötter, J. Heinze, N. Hölzel, K. Jung, V. H. Klaus, T. Kleinebecker, S. Klemmer, J. Krauss, M. Lange, E. K. Morris, J. Müller, Y. Oelmann, J. Overmann, E. Pašalić, M. C. Rillig, H. M. Schaefer, M. Schloter, B. Schmitt, I. Schöning, M. Schrumpf, J. Sikorski, S. A. Socher, E. F. Solly, I. Sonnemann, E. Sorkau, J. Steckel, I. Steffan-Dewenter, B. Stempfhuber, M. Tschapka, M. Türke, P. C. Venter, C. N. Weiner, W. W. Weisser, M. Werner, C. Westphal, W. Wilcke, V. Wolters, T. Wubet, S. Wurst, M. Fischer, E. Allan, Biodiversity at multiple trophic levels is needed for ecosystem multifunctionality. *Nature* **536**, 456–459 (2016).

13. G. E. Belovsky, J. B. Slade, Insect herbivory accelerates nutrient cycling and increases plant production. *Proc. Natl. Acad. Sci. U.S.A.* **97**, 14412–14417 (2000).

14. P. W. Price, Resource-driven terrestrial interaction webs. *Ecol. Res.* **17**, 241–247 (2002).

15. J. Bascompte, P. Jordano, Plant-animal mutualistic networks: The architecture of biodiversity. *Annu. Rev. Ecol. Evol. Syst.* **38**, 567–593 (2007).

16. L. Pellissier, C. Albouy, J. Bascompte, N. Farwig, C. Graham, M. Loreau, M. A. Maglianesi, C. J. Melián, C. Pitteloud, T. Roslin, R. Rohr, S. Saavedra, W. Thuiller, G. Woodward, N. E. Zimmermann, D. Gravel, Comparing species interaction networks along environmental gradients. *Biol. Rev.* **93**, 785–800 (2018).

17. M. A. Fortuna, D. B. Stouffer, J. Olesen, P. Jordano, D. Mouillot, B. Krasnov, R. Poulin, J. Bascompte, Nestedness versus modularity in ecological networks: Two sides of the same coin? *J. Anim. Ecol.* **79**, 811–7 (2010).

18. M. Kondoh, S. Kato, Y. Sakato, Food webs are built up with nested subwebs. *Ecology* **91**, 3123–3130 (2010).

19. S. L. Pimm, The structure of food webs. *Theor. Popul. Biol.* **16**, 144–158 (1979).

20. J. Bascompte, P. Jordano, C. J. Melián, J. M. Olesen, The nested assembly of plant-animal mutualistic networks. *Proc. Natl. Acad. Sci. U.S.A.* **100**, 9383–9387 (2003).

21. J. M. Olesen, J. Bascompte, Y. L. Dupont, P. Jordano, The modularity of pollination networks. *Proc. Natl. Acad. Sci. U.S.A.* **104**, 19891–19896 (2007).

22. B. J. Spiesman, B. D. Inouye, Habitat loss alters the architecture of plant–pollinator interaction networks. *Ecology* **94**, 2688–2696 (2013).

23. N. K. Simons, W. W. Weisser, M. M. Gossner, Multi-taxa approach shows consistent shifts in arthropod functional traits along grassland land-use intensity gradient. *Ecology* **97**, 754–764 (2016).

24. C. Song, R. P. Rohr, S. Saavedra, Why are some plant–pollinator networks more nested than others? *J. Anim. Ecol.* **86**, 1417–1424 (2017).

25. S. Macfadyen, R. H. Gibson, W. O. C. Symondson, J. Memmott, Landscape structure influences modularity patterns in farm food webs: Consequences for pest control. *Ecol. Appl.* **21**, 516–524 (2011).

26. A. J. Vanbergen, B. A. Woodcock, M. S. Heard, D. S. Chapman, Network size, structure and mutualism dependence affect the propensity for plant–pollinator extinction cascades. *Funct. Ecol.* **31**, 1285–1293 (2017).

27. S. Santamaría, A. M. Sánchez, J. López-Angulo, C. Ornosa, I. Mola, A. Escudero, Landscape effects on pollination networks in Mediterranean gypsum islands. *Plant Biol.* **20**, 184–194 (2018).

28. I. Grass, B. Jauker, I. Steffan-Dewenter, T. Tscharntke, F. Jauker, Past and potential future effects of habitat fragmentation on structure and stability of plant–pollinator and host–parasitoid networks. *Nat. Ecol. Evol.* **2**, 1408–1417 (2018).

29. B. M. L. Morrison, B. J. Brosi, R. Dirzo, Agricultural intensification drives changes in hybrid network robustness by modifying network structure. *Ecol. Lett.* **23**, 359–369 (2020).

30. E. Thébault, C. Fontaine, Stability of ecological communities and the architecture of mutualistic and trophic networks. *Science* **329**, 853–856 (2010).

31. R. M. May, Will a large complex system be stable? *Nature* **238**, 413–414 (1972).

32. J. Teng, K. S. McCann, Dynamics of compartmented and reticulate food webs in relation to energetic flows. *Am. Nat.* **164**, 85–100 (2004).

33. J. Memmott, N. M. Waser, M. V. Price, Tolerance of pollination networks to species extinctions. *Proc. Biol. Sci.* **271**, 2605–2611 (2004).

34. E. Burgos, H. Ceva, R. P. J. Perazzo, M. Devoto, D. Medan, M. Zimmermann, A. M. Delbue, Why nestedness in mutualistic networks? *J. Theoret. Biol.* **249**, 307–313 (2007).

35. M. T. Baumgartner, Connectance and nestedness as stabilizing factors in response to pulse disturbances in adaptive antagonistic networks. *J. Theor. Biol.* **486**, 110073 (2020).

36. J. A. Dunne, R. J. Williams, N. D. Martinez, Network structure and biodiversity loss in food webs: Robustness increases with connectance. *Ecol. Lett.* **5**, 558–567 (2002).

37. J. W. Redhead, B. A. Woodcock, M. J. O. Pocock, R. F. Pywell, A. J. Vanbergen, T. H. Oliver, Potential landscape-scale pollinator networks across Great Britain: Structure, stability and influence of agricultural land cover. *Ecol. Lett.* **21**, 1821–1832 (2018).

38. M. Fischer, O. Bossdorf, S. Gockel, F. Hänsel, A. Hemp, D. Hessenmöller, G. Korte, J. Nieschulze, S. Pfeiffer, D. Prati, S. Renner, I. Schöning, U. Schumacher, K. Wells, F. Buscot, E. K. V. Kalko, K. E. Linsenmair, E.-D. Schulze, W. W. Weisser, Implementing large-scale and long-term functional biodiversity research: The Biodiversity Exploratories. *Basic Appl. Ecol.* **11**, 473–485 (2010).

39. D. P. Giling, A. Ebeling, N. Eisenhauer, S. T. Meyer, C. Roscher, M. Rzanny, W. Voigt, W. W. Weisser, J. Hines, Plant diversity alters the representation of motifs in food webs. *Nat. Commun.* **10**, 1226 (2019).

40. J.-Y. Humbert, J. Ghazoul, T. Walter, Meadow harvesting techniques and their impacts on field fauna. *Agric. Ecosyst. Environ.* **130**, 1–8 (2009).

41. T. Hilmers, N. Friess, C. Bässler, M. Heurich, R. Brandl, H. Pretzsch, R. Seidl, J. Müller, Biodiversity along temperate forest succession. *J. Appl. Ecol.* **55**, 2756–2766 (2018).

42. S. Boch, D. Prati, J. Müller, S. Socher, H. Baumbach, F. Buscot, S. Gockel, A. Hemp, D. Hessenmöller, E. K. V. Kalko, K. E. Linsenmair, S. Pfeiffer, U. Pommer, I. Schöning, E.-D. Schulze, C. Seilwinder, W. W. Weisser, K. Wells, M. Fischer, High plant species richness indicates management-related disturbances rather than the conservation status of forests. *Basic Appl. Ecol.* **14**, 496–505 (2013).

43. M. M. Gossner, T. M. Lewinsohn, T. Kahl, F. Grassein, S. Boch, D. Prati, K. Birkhofer, S. C. Renner, J. Sikorski, T. Wubet, H. Arndt, V. Baumgartner, S. Blaser, N. Blüthgen, C. Börschig, F. Buscot, T. Diekötter, L. R. Jorge, K. Jung, A. C. Keyel, A.-M. Klein, S. Klemmer, J. Krauss, M. Lange, J. Müller, J. Overmann, E. Pašalić, C. Penone, D. J. Perović, O. Purschke, P. Schall, S. A.

Socher, I. Sonnemann, M. Tschapka, T. Tscharntke, M. Türke, P. C. Venter, C. N. Weiner, M. Werner, V. Wolters, S. Wurst, C. Westphal, M. Fischer, W. W. Weisser, E. Allan, Land-use intensification causes multitrophic homogenization of grassland communities. *Nature* **540**, 266–269 (2016).

44. V. H. Klaus, N. Hölzel, S. Boch, J. Müller, S. A. Socher, D. Prati, M. Fischer, T. Kleinebecker, Direct and indirect associations between plant species richness and productivity in grasslands: Regional differences preclude simple generalization of productivity-biodiversity relationships. *Preslia* **85**, 97–112 (2013).

45. N. K. Simons, M. M. Gossner, T. M. Lewinsohn, M. Lange, M. Türke, W. W. Weisser, Effects of land-use intensity on arthropod species abundance distributions in grasslands. *J. Anim. Ecol.* **84**, 143–154 (2015).

46. C. Bakker, J. M. Blair, A. K. Knapp, Does resource availability, resource heterogeneity or species turnover mediate changes in plant species richness in grazed grasslands? *Oecologia* **137**, 385–391 (2003).

47. D. G. Milchunas, O. E. Sala, W. K. Lauenroth, A generalized model of the effects of grazing by large herbivores on grassland community structure. *Am. Nat.* **132**, 87–106 (1988).

48. J. P. Grime, Control of species density in herbaceous vegetation. *J. Environ. Manage.* **1**, 151–167 (1973).

49. J. Leidinger, S. Seibold, W. W. Weisser, M. Lange, P. Schall, M. Türke, M. M. Gossner, Effects of forest management on herbivorous insects in temperate Europe. *For. Ecol. Manage.* **437**, 232–245 (2019).

50. H. Mielke, W. Wohlers, *Praxishandbuch Grünland: Nutzung und Pflege* (Agrimedia, ed. 2, 2016).

51. P. Jordano, Sampling networks of ecological interactions. *Funct. Ecol.* **30**, 1883–1893 (2016).

52. R. van Klink, F. van der Plas, C. G. E. T. van Noordwijk, M. F. WallisDeVries, H. Olff, Effects of large herbivores on grassland arthropod diversity. *Biol. Rev.* **90**, 347–366 (2015).

53. C. Ammer, Diversity and forest productivity in a changing climate. *New Phytol.* **221**, 50–66 (2019).

54. N. Blüthgen, C. F. Dormann, D. Prati, V. H. Klaus, T. Kleinebecker, N. Hölzel, F. Alt, S. Boch, S. Gockel, A. Hemp, J. Müller, J. Nieschulze, S. C. Renner, I. Schöning, U. Schumacher, S. A. Socher, K. Wells, K. Birkhofer, F. Buscot, Y. Oelmann, C. Rothenwöhrer, C. Scherber, T. Tscharntke, C. N. Weiner, M. Fischer, E. K. V. Kalko, K. E. Linsenmair, E.-D. Schulze, W. W. Weisser, A quantitative index of land-use intensity in grasslands: Integrating mowing, grazing and fertilization. *Basic Appl. Ecol.* **13**, 207–220 (2012).

55. T. Kahl, J. Bauhus, An index of forest management intensity based on assessment of harvested tree volume, tree species composition and dead wood origin. *Nat. Conserv.* **7**, 15–27 (2014).

56. P. Schall, C. Ammer, How to quantify forest management intensity in Central European forests. *Eur. J. For. Res.* **132**, 379–396 (2013).

57. P. Schall, E.-D. Schulze, M. Fischer, M. Ayasse, C. Ammer, Relations between forest management, stand structure and productivity across different types of Central European forests. *Basic Appl. Ecol.* **32**, 39–52 (2018).

58. F. Schmitz, H. Polley, P. Hennig, K. Dunger, F. Schwitzgebel, *Die zweite Bundeswaldinventur - BWI2 : Inventur- und Auswertungsmethoden* (Johann Heinrich von Thünen-Institut, 2008).

59. E. Kowalski, M. M. Gossner, M. Türke, M. Lange, D. Veddeler, D. Hessenmöller, E.-D. Schulze, W. W. Weisser, The use of forest inventory data for placing flight-interception traps in the forest canopy. *Entomol. Exp. Appl.* **140**, 35–44 (2011).

60. M. M. Gossner, U. Ammer, The effects of Douglas-fir on tree-specific arthropod communities in mixed species stands with European beech and Norway spruce. *Eur. J. For. Res.* **125**, 221–235 (2006).

61. R Core Team, *R: A Language and Environment for Statistical Computing* (R Foundation for Statistical Computing, 2018).

62. C. F. Dormann, J. Fründ, B. Gruber, *Visualising Bipartite Networks and Calculating Some (Ecological) Indices*, R package version 2.13 (2019).

63. J. S. Lefcheck, PIECEWISESEM: Piecewise structural equation modelling in R for ecology, evolution, and systematics. *Methods Ecol. Evol.* **7**, 573–579 (2016).

64. J. Pinheiro, D. Bates, S. DebRoy, D. Sarkar, EISPACK authors, S. Heisterkamp, B. Van Willigen, R Core Team, *Linear and Nonlinear Mixed Effects Models*, R package version 3.1–131 (2017).

65. J. S. Lefcheck, *Piecewise Structural Equation Modeling*, R package version 1.2.1 (2016).

66. N. P. Lemoine, Moving beyond noninformative priors: Why and how to choose weakly informative priors in Bayesian analyses. *Oikos* **128**, 912–928 (2019).

67. J. Guo, J. Gabry, D. Lee, K. Sakrejda, M. Modrák, Trustees of Columbia University, O. Sklyar, R Core Team, J. Oehlschlaegel-Akiyoshi, *R Interface to Stan*, R package version 2.18.2 (2018).

68. M. M. Gossner, N. K. Simons, R. Achtziger, T. Blick, W. H. O. Dorow, F. Dziock, F. Köhler, W. Rabitsch, W. W. Weisser, A summary of eight traits of Coleoptera, Hemiptera, Orthoptera and Araneae, occurring in grasslands in Germany. *Sci. Data* **2**, 150013 (2015).

69. J. H. Brown, J. F. Gillooly, A. P. Allen, V. M. Savage, G. B. West, Toward a metabolic theory of ecology. *Ecology* **85**, 1771–1789 (2004).

70. E. H. Sohlström, L. Marian, A. D. Barnes, N. F. Haneda, S. Scheu, B. C. Rall, U. Brose, M. Jochum, Applying generalized allometric regressions to predict live body mass of tropical and temperate arthropods. *Ecol. Evol.* **8**, 12737–12749 (2018).

71. E. H. Sohlström, L. Marian, A. D. Barnes, N. F. Haneda, S. Scheu, B. C. Rall, U. Brose, M. Jochum, Data from: Applying generalised allometric regressions to predict live body mass of tropical and temperate arthropods. *Dryad Digital Repository* (2018), doi:10.5061/dryad.vk24fr1.

72. M. Kleiber, Body size and metabolism. *Hilgardia* **6**, 315–353 (1932).

73. E. J. Jäger, F. Müller, C. M. Ritz, E. Welk, K. Wesche, *Rothmaler – Exkursionsflora von Deutschland. Gefäßpflanzen: Atlasband* (Springer-Verlag, ed. 13, 2017).

74. A. Bolte, "Biomasse- und Elementvorräte der Bodenvegetation auf Flächen des forstlichen Umweltmonitorings in Rheinland-Pfalz (BZE, EU Level II)," in *Berichte des Forschungszentrums Waldökosysteme, Reihe B* , vol 72, F. Beese, Ed. (Forschungszentrum Waldökosysteme der Universität Göttingen, 2006).

75. A. Bolte, T. Czajkowski, J. Bielefeldt, B. Wolff, S. Heinrichs, Schätzung der oberirdischen Biomassevorräte des Baum- und Strauchunterwuchses in Wäldern auf der Basis von Vegetationsaufnahmen. *Forstarchiv* **80**, 222–228 (2009).

76. D. I. Forrester, I. H. H. Tachauer, P. Annighoefer, I. Barbeito, H. Pretzsch, R. Ruiz-Peinado, H. Stark, G. Vacchiano, T. Zlatanov, T. Chakraborty, S. Saha, G. W. Sileshi, Generalized biomass and leaf area allometric equations for European tree species incorporating stand structure, tree age and climate. *For. Ecol. Manage.* **396**, 160–175 (2017).

77. H. Nickel, *The Leafhoppers and Planthoppers of Germany (Hemiptera, Auchenorrhyncha): Patterns and Strategies in a Highly Diverse Group of Phytophagous Insects* (Pensoft/Goecke & Evers, 2003).

78. N. Loeuille, S. Barot, E. Georgelin, G. Kylafis, C. Lavigne, Eco-evolutionary dynamics of agricultural networks: Implications for sustainable management. *Adv. Ecol. Res.* **49**, 339–435 (2013).

79. R. Biedermann, R. Niedringhaus, *Die Zikaden Deutschlands - Bestimmungstafeln für alle Arten* (Wissenschaftlich Akademischer Buchvertrieb-Fründ, 2004).

80. J. Burmeister, M. Goßner, A. Gruppe, Insektengemeinschaften im Kronenraum von Koniferenarten im Forstlichen Versuchsgarten Grafrath. *Nachr. Bayer. Entomol.* **56**, 19–29 (2007).

81. V. Derjanschi, J. Péricart, *Hémiptères Pentatomoidea euro-méditerranéens - Volume 1, Généralités, systématique: première partie*, vol. 90 of *Faune de France* (Fédération Française des Sociétés de Sciences Naturelles, 2005).

82. W. N. Ellis, Plant Parasites of Europe – leafminers, galls and fungi (2001–2020); www.bladmineerders.nl/.

83. J. Gorczyca, *A catalogue of plant bugs (Heteroptera: Miridae) of Poland. Part I. Subfamilies: Isometopinae, Deraeocorinae, Bryocorinae, Orthotylinae, Phylinae* (Natura Optima dux Foundation, 2007).

84. M. M. Gossner, Diversität und Struktur arborikoler Arthropodenzönosen fremdländischer und einheimischer Baumarten. Ein Beitrag zur Bewertung des Anbaus von Douglasie (*Pseudotsuga menziesii* (Mirb.) Franco) und Roteiche (*Quercus rubra* L.). *Neobiota.* **5**, 1–324 (2004).

85. M. M. Goßner, A. Gruppe, U. Simon, Aphidophagous insect communities in tree crowns of the neophyte Douglas-fir [*Pseudotsuga menziesii* (Mirb.) Franco] and Norway spruce (*Picea abies* L.). *J. Appl. Entomol.* **129**, 81–88 (2005).

86. M. M. Gossner, The importance of Silver fir (*Abies alba* Mill.) in comparison to spruce (*Picea abies* (L.) Karst.) and oak (*Quercus petraea* (Matt.) Liebl.) for arboreal Heteroptera communities in Bavarian forests. *Waldoekologie Online* **2**, 90–105 (2005).

87. M. M. Goßner, M. Bräu, Die Wanzen der Neophyten Douglasie (Pseudotsuga menziesii) und Amerikanischer Roteiche (Quercus rubra) im Vergleich zur Fichte und Tanne bzw. Stieleiche und Buche in südbayerischen Wäldern – Schwerpunkt arborikole Zönosen. *Beiträge zur bayerischen Entomofaunistik* **6**, 217–235 (2004).

88. E. Heiss, J. Péricart, *Hémiptères Aradidae, Piesmatidae et Dipsocoromorphes*, vol. 91 of *Faune de France* (Fédération Française des Sociétés de Sciences Naturelles, 2007).

89. J. K. Holopainen, A.-L. Varis, Host plants of the European tarnished plant bug *Lygus rugulipennis* Poppius (Het., Miridae). *J. Appl. Entomol.* **111**, 484–498 (1991).

90. P. Moulet, *Hémiptères Coreoidea (Coreidae, Rhopalidae, Alydidae) Pyrrhocoridae, Stenocephalidae Euro-Méditerranéens*, vol. 81 of *Faune de France* (Fédération Française des Sociétés de Sciences Naturelles, 1995).

91. J. Péricart, *Hémiptères Berytidae Euro-Méditerranéens*, vol. 70 of *Faune de France* (Fédération Française des Sociétés de Sciences Naturelles, 1984).

92. J. Péricart, *Hémiptères Lygaeidae Euro-Méditerranéens*, vol. 84 of *Faune de France* (Fédération Française des Sociétés de Sciences Naturelles, 1998).

93. J. Ribes, S. Pagola-Carte, *Hémiptères Pentatomoidea Euro-Méditerranéens - Volume 2, Systématique: Deuxième Partie, Sous-Famille Pentatominae (Suite et Fin)*, vol. 96 of *Faune de France*, (Fédération Française des Sociétés de Sciences Naturelles, 2013).

94. T. Rintala, V. Rinne, *Suomen Luteet* (Hyönteistarvike Tibiale Oy, 2010).

95. L. Skipper, *Danmarks Blomstertæger*, vol. 12 of *Danmarks Dyreliv* (Apollo Booksellers, 2013).

96. E. Wachmann, A. Melber, J. Deckert, *Wanzen Band 1-5* (Goecke & Evers, 2004–2012).

97. E. Wagner, H.-H. Weber, *Hétéroptères Miridae* vol. 67 of *Faune de France* (Fédération Française des Sociétés de Sciences Naturelles, 1964).

98. U. Bense, *Longhorn Beetles: Illustrated Key to the Cerambycidae and Vesperidae of Europe* (Margraf, 1995).

99. J. Böhme, *Katalog (faunistische Übersicht)*, vol. K of *Die Käfer Mitteleuropas* (Springer Spektrum, ed. 2, 2005).

100. P. Brandmayr, T. Zetto Brandmayr, Identificazione di larve del genere Ophonus Dejean, 1821 (sensu novo) e note bionomiche. *Mem. Soc. Ent. Ital.* **60**, 67–103 (1981).

101. T. Brandmayr Zetto, in *The Role of Ground Beetles in Ecological and Environmental Studies*, N. E. Stork, Ed. (Intercept, 1990), pp. 307–316.

102. L. Dieckmann, Beiträge zur Insektenfauna der DDR: Coleoptera - Curculionidae: Ceutorhynchinae. *Beitr. Entomol.* **22**, 3–128 (1972).

103. L. Dieckmann, Beiträge zur Insektenfauna der DDR: Coleoptera - Curculionidae Brachycerinae, Otiorhynchinae. *Beitr. Entomol.* **30**, 145–310 (1980).

104. L. Dieckmann, Beiträge zur Insektenfauna der DDR: Coleoptera - Curculionidae (Erirhinae). *Beitr. Entomol.* **36**, 119–181 (1986).

105. H. Freude, K. W. Harde, G. A. Lohse, *Die Käfer Mitteleuropas Band 1-15* (Goecke & Evers, 1965–1998).

106. B. Klausnitzer, H. Klausnitzer, *Marienkäfer: Coccinellidae*, vol. 451 of *Die Neue Brehm-Bücherei* (Westarp Wissenschaften, ed. 4, 1997).

107. K. Koch, *Die Käfer Mitteleuropas - Ökologie Band 1-3* (Goecke & Evers, 1989–1992).

108. A. Pfeffer, *Zentral- und Westpaläarktische Borken- und Kernkäfer (Coleoptera, Scolytidae, Platypodidae)*, vol. 17 of *Entomologica Basiliensia* (Pro Entomologia, 1995).

109. J. Rheinheimer, M. Hassler, *Die Rüsselkäfer Baden-Württembergs*, vol. 99 of *Naturschutz-Spectrum. Themen* (Verlag Regionalkultur, 2010).

110. J. Rheinheimer, M. Hassler, *Die Blattkäfer Baden-Württembergs* (Kleinsteuber Books, 2018).

111. B. Baur, H. Baur, C. Roesti, D. Roesti, *Die Heuschrecken der Schweiz* (Haupt Verlag, 2006).

112. S. Ingrisch, G. Köhler, *Die Heuschrecken Mitteleuropas*, vol. 629 of *Die Neue Brehm-Bücherei* (Westarp Wissenschaften, 1998).

113. H. Schlumprecht, G. Waeber, *Heuschrecken in Bayern* (Verlag Eugen Ulmer, 2003).